THE ASTROPHYSICAL JOURNAL, 527:180–198, 1999 December 10

HALO STAR LITHIUM DEPLETION

M. H. PINSONNEAULT,[1] T. P. WALKER,[1,2] G. STEIGMAN,[1,2] AND VIJAY K. NARAYANAN[1]
Ohio State University, Columbus, OH 43210
Received 1998 March 6; accepted 1999 July 23

ABSTRACT

The depletion of lithium during the pre–main-sequence and main-sequence phases of stellar evolution plays a crucial role in the comparison of the predictions of big bang nucleosynthesis with the abundances observed in halo stars. Previous work has indicated a wide range of possible depletion factors, ranging from minimal in standard (nonrotating) stellar models to as much as an order of magnitude in models that include rotational mixing. Recent progress in the study of the angular momentum evolution of low-mass stars permits the construction of theoretical models capable of reproducing the angular momentum evolution of low-mass open cluster stars. The distribution of initial angular momenta can be inferred from stellar rotation data in young open clusters. In this paper we report on the application of these models to the study of lithium depletion in main-sequence halo stars. A range of initial angular momenta produces a range of lithium depletion factors on the main sequence. Using the distribution of initial conditions inferred from young open clusters leads to a well-defined halo lithium plateau with modest scatter and a small population of outliers. The mass-dependent angular momentum loss law inferred from open cluster studies produces a nearly flat plateau, unlike previous models that exhibited a downward curvature for hotter temperatures in the ^{7}Li-$T_{\rm eff}$ plane. The overall depletion factor for the plateau stars is sensitive primarily to the solar initial angular momentum used in the calibration for the mixing diffusion coefficients. Uncertainties remain in the treatment of the internal angular momentum transport in the models, and the potential impact of these uncertainties on our results is discussed. The ^{6}Li/^{7}Li depletion ratio is also examined. We find that the dispersion in the plateau and the ^{6}Li/^{7}Li depletion ratio scale with the absolute ^{7}Li depletion in the plateau, and we use observational data to set bounds on the ^{7}Li depletion in main-sequence halo stars. A maximum of 0.4 dex depletion is set by the observed dispersion and ^{6}Li/^{7}Li depletion ratio, and a minimum of 0.2 dex depletion is required by both the presence of highly overdepleted halo stars and consistency with the solar and open cluster ^{7}Li data. The cosmological implications of these bounds on the primordial abundance of ^{7}Li are discussed.

Subject headings: Galaxy: halo — stars: abundances — stars: evolution — stars: interiors

1. INTRODUCTION

The status of big bang nucleosynthesis (BBN) as a cornerstone of the hot big bang cosmology rests on the agreement between the theoretical predictions and the primordial abundances of the light elements deuterium (D), helium 3 (^{3}He), helium 4 (^{4}He), and lithium 7 (^{7}Li) inferred from observational data (Yang et al. 1984; Walker et al. 1991; Copi, Schramm, & Turner 1995a). Comparisons of this type often rely on models of Galactic chemical and/or stellar evolution in order to associate the observed abundances of these light elements at the present epoch with their predicted primordial values. Recently the confrontation between prediction and observation has come under stricter scrutiny as it appeared that the primordial abundance of deuterium inferred from ISM/solar data (Dring et al. 1997) was smaller than its predicted abundance—the value of which follows from requiring that the standard big bang model predictions for ^{4}He are in good agreement with the abundance inferred from observations of metal-poor extragalactic H II regions (Hata et al. 1995; Copi, Schramm, & Turner 1995b; Hata et al. 1997). Very recent measurements of the deuterium abundance along the lines of sight to high-redshift QSOs (Burles & Tytler 1997), along with a reanalysis of the ^{4}He data in light of new observations (Olive, Skillman, & Steigman 1997), increase the tension between prediction and observation.

The role of ^{7}Li in these comparisons has been minor because of the large uncertainty in the estimate of the amount of lithium destruction during the lifetimes of Population II (i.e., metal poor) halo stars that could accommodate primordial lithium abundances ranging from the observed plateau value[3] (no depletion) up to a factor of 10 larger. This range in possible depletion factors is equally compatible with primordial lithium abundances that correspond to either "low deuterium" (which favors a primordial lithium abundance a factor of 3 higher than the plateau value) or the observed ^{4}He (which favors the plateau value).

The arguments in favor of minimal lithium depletion are the flatness of the Population II lithium abundance plateau (at low metallicity and high temperature) with respect to both metallicity and temperature and the low dispersion in the lithium abundance at fixed $T_{\rm eff}$. This was generally consistent with "standard" stellar models (i.e., models without rotation that burn lithium via convection during pre–main-sequence evolution), which predicted little depletion (Deliyannis et al. 1989). There are however some specific areas of disagreement in the comparison of the halo star data with standard models. The observed dispersion may be greater than that predicted (Deliyannis, Pinsonneault, & Duncan 1993; Thorburn 1994; Ryan et al. 1996) or not (Molaro, Primas, & Bonifacio 1995; Spite et al. 1996). There

[1] Department of Astronomy, Ohio State Univerity.
[2] Department of Physics, Ohio State University.

[3] The lithium abundances of Population II stars with $T_{\rm eff} > 5800$ K and [Fe/H] < -1.3 are nearly independent of metallicity ([Li] $= 2.25 \pm 0.1$, where $[X] = 12 + \log y_X$ with y_X the number ratio of X to hydrogen) and, hence, are referred to as a "plateau." See § 4.1 for a discussion of the observational data.

is a small population of highly overdepleted stars that appear normal except for ^{7}Li (Thorburn 1994; Norris et al. 1997). In addition, the trends with metal abundance appear to conflict with expectations from the models (Thorburn 1994; Chaboyer & Demarque 1994), although there is some controversy over the reality of the trends in the observational data (see § 3.3.1). However, the overall agreement between standard (no rotation, no gravitational settling or thermal diffusion, and no mass loss) stellar evolution theory and observations in halo stars is good enough that nonstandard models would probably not be invoked to explain this data set. Therefore many investigators have adopted the reasonable assumption that the observed Population II lithium abundances are close to the primordial value. We note, however, that the application of standard models to the problem of lithium depletion encounters significant difficulties with both the full set of observational data and advances in our understanding of physical processes neglected in standard models, notably microscopic diffusion and rotational mixing.

The overall properties of ^{7}Li depletion in standard models have been extensively studied (for a review see Pinsonneault 1997) and there are some model-independent predictions: there is partial ^{7}Li depletion in the pre–main sequence (pre-MS), little or no main-sequence (MS) depletion for stars hotter than about 5500 K, and little or no dispersion in the ^{7}Li abundance at a given $T_{\rm eff}$ in clusters. Unfortunately, the observational data obtained from halo stars does not serve as a good diagnostic for these models since we have no information on the history of the ^{7}Li abundance. Instead, one can look to the Sun and open clusters, systems with a nearly uniform initial lithium abundance ([Li] = 3.2–3.4) for which detailed abundance data is available as a function of mass, age, and composition. These Population I data provide stringent tests of theoretical models, and it has been known for quite some time (e.g., see Weyman & Sears 1965; Zappala 1972) that standard models fail these tests. The disagreement between the data and standard models has increased as both the observational data and the standard theoretical models have improved. The open cluster data provide clear evidence that the ^{7}Li abundance decreases with increasing age on the MS, contrary to the standard model prediction that the convective zones of these hot ($\geq$5500 K) stars are not deep enough to destroy ^{7}Li on the MS. In addition, there is strong evidence for a dispersion in abundance at fixed $T_{\rm eff}$ and unexpected mass-dependent effects, such as the strong depletion seen in mid-F stars relative to both hotter and cooler stars (the "Li dip" of Boesgaard & Trippico 1986—for extensive reviews of this issue, see Pilachowski & Hobbs 1988; Michaud & Charbonneau 1991; Soderblom 1995; Balachandran 1995; Pinsonneault 1997). For standard models, these features cannot be explained by variations in the input physics (e.g., opacities); rather, they indicate the operation of physical processes not usually included in standard models. By extension, these processes could also be operating in the Population II stars.

Another potentially useful diagnostic of lithium depletion can be found in globular clusters. Clusters provide samples that are homogeneous in age and composition, so one would expect a smaller dispersion in a cluster sample than in a field star sample. This is certainly the case for Population I stars: Population I field stars do show a larger dispersion than open cluster stars (Lambert, Heath, & Edvardsson 1991; Favata, Micela, & Sciortino 1996). However, recent observations of Li in globular cluster subgiant and turnoff stars show the opposite trend and create some serious difficulties for the minimal ^{7}Li depletion scenario for metal poor stars. There are clear star-to-star differences in M92 (Deliyannis, Boesgaard, & King 1995; Boesgaard et al. 1998); of three stars with very similar color observed, two have lithium abundances well below the plateau value. In NGC 6397, 20 stars near the turnoff were observed (Thorburn et al. 1997). For seven with identical $B-V$ color, there is a scatter of a factor of 2–3 in lithium abundance (see also Pasquini & Molaro 1996 for a discussion of a smaller sample). Therefore a standard model treatment of the halo field stars must explain why the lithium abundances in globular clusters, but not in field stars, are anomalous.

The disagreement between the Population I lithium abundances and the predictions of standard stellar models has stimulated investigation of various nonstandard stellar models. "Nonstandard" does not imply "speculative"; in fact, there are solid physical grounds for including several effects neglected in the standard stellar model. The most prominent explanations are mixing (either from rotation or waves), microscopic diffusion, and mass loss (Pinsonneault 1997; Michaud & Charbonneau 1991). For Population I G and K stars, microscopic diffusion and mass loss do not explain the overall lithium depletion pattern (Michaud & Charbonneau 1991; Swenson & Faulkner 1992), which leaves mixing as a logical candidate. Mixing induced by rotation can explain many of the overall properties of the Population I data. Rotational mixing can, on relatively long timescales, mix material from the base of the convective zone to interior regions of the star where lithium can be burned; both the rotation rate and the ^{7}Li depletion rate decrease with increased age; and a distribution of initial rotation rates can produce a distribution of ^{7}Li depletions and thus a dispersion in abundance at fixed $T_{\rm eff}$.

Although models with rotational mixing have the qualitative properties needed to explain the Population I and Population II data, two classes of objections have been raised, based on (1) the uniqueness of the solutions and adequacy of the physical model and (2) discrepancies in the quantitative comparison of observation and theory. Rotational models require an understanding of the angular momentum as a function of radius and as a function of time. There have been persistent difficulties in reproducing the surface rotation rates as a function of mass and time in open clusters (Chaboyer, Demarque, & Pinsonneault 1995a, 1995b; Keppens, MacGregor, & Charbonneau 1995; Bouvier 1994). In addition, models with internal angular momentum transport from hydrodynamic mechanisms, such as the ones used in this paper, predict more rapid core rotation in the Sun than is compatible with helioseismology data (Chaboyer et al. 1995a; Krishnamurthi et al. 1997a, hereafter KPBS; Tomczyk, Schou, & Thompson 1995). Either of these difficulties could potentially affect the degree of mixing in the models.

Models with rotational mixing predict that a range of initial angular momenta will generate a range of lithium depletion rates and therefore a dispersion in abundance among stars of the same mass, composition, and age. However, the difficulty in reproducing the angular momentum evolution of low-mass stars has made quantifying the predicted dispersion difficult, and therefore only qualitative

estimates have been made (e.g., see Pinsonneault, Kawaler, & Demarque 1990, hereafter PKD; Chaboyer & Demarque 1994; Chaboyer et al. 1995b; Charbonnel, Vauclair, & Zahn 1992). There have also been mismatches between the mean trend inferred from the data and from all classes of theoretical models. Chaboyer & Demarque (1994), for example, concluded that the observed mean trend of lithium abundance with $T_{\rm eff}$ in metal-poor halo stars was not reproduced in *any* class of models, be they standard, rotational, or with diffusion. There are also cases, such as the cool stars in young open clusters, in which the observed dispersion is large but the rotational models predict little, if any, dispersion.

The case for or against standard model lithium depletion is not as clear cut when we consider halo stars. It is argued that models with significant rotationally induced depletion could not produce a flat plateau with limited dispersion about the mean plateau abundance (e.g., Bonifacio & Molaro 1997). Furthermore, it was expected that such models would destroy far too much ^{6}Li (Steigman et al. 1993), in conflict with the observation of ^{6}Li in HD 84937 (see § 4.2). On the other hand, standard (convective burning) models show lithium depletion trends contrary to the Population I data and they neglect physical processes that are both physically based and required by other observational data, such as helioseismology.

At a minimum, the mechanisms responsible for the Population I ^{7}Li pattern need to be identified and shown to not affect Population II stars. It is difficult to construct a model in which the nonstandard effects completely cancel for Population II stars while still retaining consistency with the Population I data. Models with microscopic diffusion predict modest ^{7}Li depletion in plateau halo stars. In general these same models predict that the timescale for changes in the surface ^{7}Li abundance decreases with increased mass; this produces a downward curvature in the ^{7}Li-$T_{\rm eff}$ relationship at high temperatures, which is not observed. Mass loss can counteract this trend (Swenson 1995; Vauclair & Charbonnel 1995). In either case, the net effect is modest depletion at the 0.2 dex level. Rotational mixing can also suppress diffusion (Chaboyer & Demarque 1994; Vauclair & Charbonnel 1995). The cancellation of different effects still requires at least some mean ^{7}Li depletion in the halo stars.

In a recent paper Vauclair & Charbonnel (1998) note that, although the surface ^{7}Li abundance varies strongly with mass in diffusive models, the peak subsurface abundance does not. They then use the height of that peak to constrain the absolute ^{7}Li abundance. It is further argued that, because the plateau dispersion is small and the plateau ^{7}Li abundance exhibits little dependence on temperature, the surface abundance must be very close to the peak subsurface abundance. Although these properties limit the degree of depletion, they do not require that it be restricted to the very small value proposed by Vauclair & Charbonnel (1998). In this paper we present models that have both of the above properties while depleting ^{7}Li to a level below the peak subsurface abundance. Chaboyer & Demarque (1994) showed that models with rotational mixing combined with diffusion had properties similar to those constructed with rotational mixing alone, indicating that these properties can be preserved in models that include both effects.

In our view the most serious source of uncertainty in models with rotational mixing has been the understanding of the angular momentum evolution of low-mass stars. We will show that many of the difficulties in reconciling observation and theory are resolved when models that are consistent with the rotation data in open clusters are used. In order to make definitive predictions of the amount of rotational mixing, it is necessary to follow the stellar angular momentum histories, which requires knowledge of the initial distribution of rotation velocities along with an angular momentum loss law. There has been significant recent progress in constructing theoretical models consistent with the rotation data in young open clusters (KPBS; Collier-Cameron & Li 1994; Keppens, MacGregor, & Charbonneau 1995; Bouvier, Forestini, & Allain 1997; Allain 1998). There has also been progress in theoretical studies of angular momentum evolution including internal gravity waves and angular momentum transport by magnetic fields (Zahn, Talon, & Matias 1997; Talon & Zahn 1997; Barnes, Charbonneau, & MacGregor 1999). With the latest generation of models, we can both infer the distribution of initial conditions and place strong constraints on the surface rotation as a function of time. This enables us to quantify the expected dispersion in lithium abundance and greatly reduces the sensitivity of the model predictions to uncertainties in the input physics. Those models that accurately reproduce the lithium abundances observed in open clusters can then be used to predict lithium depletion in halo stars. The general trend is that these "open-cluster–normalized" rotation models for halo stars predict more lithium depletion than do the standard models but less depletion than predicted by earlier studies of rotational mixing with less sophisticated treatment of angular momentum evolution.

Our goal in this paper is to constrain the amount of lithium depletion in Population II stars using several observables: (1) an estimate of the halo star initial rotation rate distribution as derived from open clusters, (2) the absence of large dispersion in the observed lithium abundances of the Population II "plateau" stars, and (3) the ^{6}Li abundance and/or the ^{6}Li/^{7}Li abundance ratio in HD 84937. We argue that, individually and in combination, these observables point to Population II halo star lithium depletion of at least 0.2 dex (following from the open cluster data) but not more than 0.4 dex (a consequence of the narrowness of the plateau and of the ^{6}Li considerations). Based on the observational data we can then infer the primordial lithium abundance and compare and contrast it with that predicted by standard BBN for consistency with the inferred primordial abundances of D and/or ^{4}He.

2. METHOD AND COMPARISON WITH PREVIOUS MODELS

2.1. *Angular Momentum Evolution and Rotational Mixing*

In standard stellar models, lithium depletion is a strong function of mass and composition; it also depends on the input physics, particularly the opacities and model atmospheres used to specify the surface boundary condition. In our models the standard model physics is the same as described in KPBS: namely, interior opacities from OPAL (Roger & Iglesias 1992); low-T opacities and model atmospheres at solar abundance from R. L. Kurucz (1991, private communication; Kurucz 1991); nuclear reaction rates from Bahcall, Pinsonneault, & Wasserberg (1995), including the Caughlin & Fowler (1988) ^{7}Li(p, α) cross section; the Yale equation of state; a solar-calibrated

mixing length, and $Y = 0.235$. Chaboyer & Demarque (1994) noted that unusual Li-$T_{\rm eff}$ trends for cool metal-poor stars occurred in models using the Kurucz atmospheres and could be lessened by using a gray atmosphere. This was traced to the Kurucz atmospheres not having a full grid of data for surface gravities and effective temperatures appropriate for the cool halo models. We therefore ran halo star models with gray atmospheres and a mixing length of 1.25 as obtained for solar models constructed under the same assumptions.

Stellar models that include rotational mixing require additional input physics beyond standard stellar models. The important new ingredients include:

1. a distribution of initial angular momenta,
2. a prescription for angular momentum loss,
3. a prescription for the internal transport of angular momentum and the associated mixing in radiative regions, and
4. the impact of rotation on the structure of the model.

There have been important changes in the treatment of the first three ingredients since the study of rotational mixing in halo dwarfs by Pinsonneault, Deliyannis, & Demarque (1992, hereafter PDD); in this section we discuss the ingredients of the current set of models and compare them with previous work. The treatment of angular momentum evolution in this set of models is the same as KPBS. The structural effects of rotation have been computed using the method of Kippenhahn & Thomas (1970) and are small for low-mass stars that experience angular momentum loss.

2.1.1. *Initial Angular Momentum*

The studies of lithium depletion in the presence of rotationally induced mixing by Pinsonneault et al. (1989, hereafter PKSD; the Sun), PKD (open cluster stars), and PDD (halo stars) all used a range of initial rotation rates in the pre-MS from the measured rotation velocities of young T Tauri stars (10–60 km s^{-1}) at a typical reference age of 1 Myr. No interaction between accretion disks and the protostar was included; the entire range of initial conditions was generated from the range in the initial rotation velocity. This caused some difficulty in reproducing the observed range in rotation (a factor of 20 in young open clusters), especially since the higher angular momentum loss rate in rapid rotators acted to reduce the range in initial rotation rates. This approach was also used by Chaboyer et al. (1995a, 1995b) for the Sun and open cluster stars, respectively, and by Chaboyer & Demarque (1994) for halo stars, although these papers used a different angular momentum loss law than the earlier work.

As protostars evolve their moments of inertia decrease; this would produce an increase in rotation rate with decreased luminosity. In contrast, the rotation periods of classical T Tauri stars appear to be nearly uniform—they do not scale with luminosity as they would if the stars were conserving angular momentum as they contracted toward the main sequence (Bouvier et al. 1993; Edwards et al. 1993). Weak-lined T Tauri stars, which are thought to be protostars without significant accretion disks, have much shorter rotation periods. This behavior would be expected if there was an accretion disk regulating the rotation of the central object and spin-up occurred only when the disk was no longer magnetically coupled to the protostar (Konigl 1991; Cameron, Campbell, & Quaintrele 1995; Keppens, MacGregor, & Charbonneau 1995). In this revised picture there is a constant surface rotation rate while there is a sufficiently massive disk around the central object. Stars that detach from their disks earlier experience a larger change in angular velocity as they contract to the main sequence than those that detach from their disk later (and are free to begin to spin up only when their moment of inertia is smaller). This disk-locking hypothesis leads to a larger range in rotation rates for models of young open cluster stars, in better agreement with the data, and explains the very slow rotation of the majority of young stars (Bouvier et al. 1997; Cameron et al. 1995; Keppens, MacGregor, & Charbonneau 1995; KPBS). These differences in the initial conditions lead to interesting consequences for the lithium depletion pattern. Although the initial rotation periods are comparable to those used in the earlier studies, the inclusion of star-disk coupling implies that the MS angular momentum is much lower for models with long disk lifetimes than it would be if the disks were absent. Disk lifetimes of 3 Myr are needed to match the rotation rates of the slow rotators in young clusters. The mean depletion for the majority of stars is therefore significantly lower than in previous studies because most young stars are slow rotators and the degree of mixing decreases for models with lower MS angular momentum.

2.1.2. *Angular Momentum Loss*

PKSD, PKD, and PDD all used a loss law of the form $dJ/dt \propto \omega^3$, where ω is the angular velocity (Kawaler 1988). This implies greater angular momentum loss for rapid rotators than for slow rotators. However, models of this type do not reproduce the rapid rotators seen in young open clusters; the spin-down of high angular momentum objects is too severe (PKD). On both theoretical and observational grounds, a more realistic functional form for the loss law is

$$\frac{dJ}{dt} \propto \omega^3 \quad (\omega < \omega_{\rm crit}) \tag{1}$$

and

$$\frac{dJ}{dt} \propto \omega\omega_{\rm crit}^2 \quad (\omega > \omega_{\rm crit}) \tag{2}$$

(MacGregor & Brenner 1991; Cameron et al. 1995; Mestel 1984; Barnes & Sofia 1996). Here $\omega_{\rm crit}$ is the angular velocity at which the angular momentum loss rate saturates; $\omega_{\rm crit}$ can be estimated from several observable quantities, thought to be correlated with surface magnetic field strength, which saturate at 5–20 times the solar rotation period (for reviews and discussions of recent work, see Patton & Simon 1996; Krishnamurthi et al. 1997). A loss law that saturates at high rotation rates allows rapid rotation to survive into the early main-sequence phase; a loss law of this form was adopted by Chaboyer et al. (1995a, 1995b) and Chaboyer & Demarque (1994).

The observational data indicate that the duration of the rapid rotator phase is a function of mass in the sense that rapid rotation survives longer in lower mass stars (for discussions, see Stauffer et al. 1997; Krishnamurthi et al. 1997). There is also indirect observational evidence for a mass-dependent saturation threshold (Patton & Simon 1996; Krishnamurthi et al. 1998). Models in which the saturation threshold scales with the convective-overturn timescale can reproduce the observed mass-dependent spin-down pattern.

We adopt the mass-dependent saturation threshold of KPBS,

$$\omega_{\rm crit} = \omega_{\rm crit}(\odot)\,\frac{\tau_{\rm conv}(\odot)}{\tau_{\rm conv}(*)}\,, \qquad (3)$$

where the convective overturn timescale $\tau_{\rm conv}$ as a function of zero-age main-sequence (ZAMS) $T_{\rm eff}$ was taken from the 200 Myr isochrones of Kim & Demarque (1996, hereafter KD). KD considered only models at solar abundance, and we would need to recalibrate the KPBS models if we used a time- and abundance-dependent overturn timescale for the models. A comparison of the convection zone depth (as a function of $T_{\rm eff}$, Z, and age) in the tables of PKD and PDD indicates that at young ages the convection zone depth at a given $T_{\rm eff}$, and therefore the overturn timescale, depends only weakly on metal abundance. The value of $\omega_{\rm crit}$ is important primarily in the early main sequence. We therefore evolved standard halo star models to an age of 200 Myr and used the same $\tau_{\rm conv}$ as a function of $T_{\rm eff}$ for the metal-poor models as reported by KD for the solar abundance models. We will consider models with a mass-, composition-, and time-dependent overturn timescale in a future paper now in preparation (Narayanan et al. 1999). A loss law with a mass-dependent saturation threshold acts preferentially to suppress rapid rotation in the more massive stars, unlike the constant saturation threshold adopted by Chaboyer & Demarque (1994). This reduces both the absolute depletion and the dispersion of lithium abundances in hotter halo plateau stars relative to cooler plateau stars.

2.1.3. *Angular Momentum Transport*

The treatment of angular momentum transport is the same as in KPBS; a detailed review of the timescale estimates can be found in Pinsonneault (1997). We consider internal angular momentum transport by hydrodynamic mechanisms alone and do not include potentially important mechanisms such as gravity waves (Kumar & Quartaret 1997; Zahn et al. 1997) and magnetic fields (Charbonneau & MacGregor 1992, 1993; Barnes et al. 1999). In previous work the degree of mixing was found to be insensitive to the assumptions about internal angular momentum transport (PKD; PDD; Chaboyer et al. 1995a, 1995b). Charbonnel et al. (1992) and Richard et al. (1996) obtained similar depletion patterns in models with solid body rotation, and Barnes et al. (1999) reported similar results in models with magnetic fields and hydrodynamic mechanisms. This can be understood because the diffusion coefficients for angular momentum transport are actually largely determined by the balance between the surface boundary condition (the applied torque) and the flux of angular momentum from below a given shell.

This is the primary reason why the amount of mixing is insensitive to the timescale for angular momentum transport: the model settles on a level of differential rotation that is needed to carry the local angular momentum flux. The opposite limiting case would be solid body rotation at all times. If we restrict ourselves to models that reproduce the observed surface rotation as a function of time, the two cases will be equivalent at the base of the surface convection zone (because the two cases will have the same distortion from spherical symmetry for the same surface rotation rate) and the diffusion coefficients for mixing will drop off more rapidly as a function of depth in the solid body case. Because ^{7}Li and ^{6}Li are destroyed relatively close to the surface convection zone, even in halo star models, the net effect will be modest; however, a suppressed degree of beryllium and boron depletion is likely in models with additional angular momentum transport mechanisms (see Barnes et al. 1999 for an example). There may also be a mass-dependent effect, in the sense of lower ^{7}Li depletion for higher mass models and a decrease in ^{7}Li depletion relative to ^{6}Li depletion.

Theory gives an estimate of the ratio of the diffusion coefficients for mixing to those for angular momentum, which is related to the existence of anisotropic turbulence in stellar interiors (Chaboyer & Zahn 1992). The diffusion coefficients for mixing are calibrated on the Sun, but our lack of information on the rotational history of the Sun requires an exploration of models with varying solar initial conditions. Specifically, we require that a solar model have the solar radius, luminosity, mean surface rotation rate, and ratio of photospheric to meteoritic lithium abundance at the age of the Sun. These conditions are used to determine the mixing length, initial helium abundance, scaling constant in the angular momentum loss law, and ratio of the diffusion coefficients for mixing to those for angular momentum transport, respectively. Only the model ^{7}Li depletion is sensitive to the solar disk lifetime.

3. RESULTS

3.1. *Initial Conditions and Angular Momentum Evolution*

We have taken the Pleiades $v \sin i$ data used in KPBS and applied a statistical correction of $4/\pi$ to all of the data points to correct for inclination angle effects. A grid of solar composition models with a range of accretion disk lifetimes was constructed and evolved to the age of the Pleiades. We interpolated in the grid to map the distribution of measured rotation velocities onto a distribution of accretion disk lifetimes. A histogram of the number of stars as a function of disk lifetimes is presented in Figure 1*a*. This distribution of initial conditions was used to infer the distribution of lithium depletion factors for different solar disk lifetimes in all of the following discussion. We then generated a grid of halo star models using the same input physics; we compare the rotation velocities of Pleiades stars to those for halo composition stars with the same disk lifetimes in Figure 1*b*. The distribution of initial conditions will be important for the remainder of our results, so we begin by discussing the properties of the Pleiades sample first. We then compare the angular momentum properties of our halo and solar abundance models.

3.1.1. *Distribution of Initial Conditions*

The measured rotation rates in the Pleiades are subject to ambiguity because we measure $v \sin i$ rather than the true rotation rate; the true rotation velocities will therefore be higher on average than the $v \sin i$ values. In addition, there are a significant number of upper limits in the data set; this technique would therefore miss any population of very slow rotators. Such stars, if present, would have less lithium depletion than our technique would permit, and they would therefore influence the predicted range in lithium depletion factors. Finally, there is the possibility that the distribution of initial conditions could depend on environment, i.e., the assumption that halo stars had the same distribution of disk lifetimes as the Pleiades, or that the Pleiades is the same as other open clusters, may be incorrect.

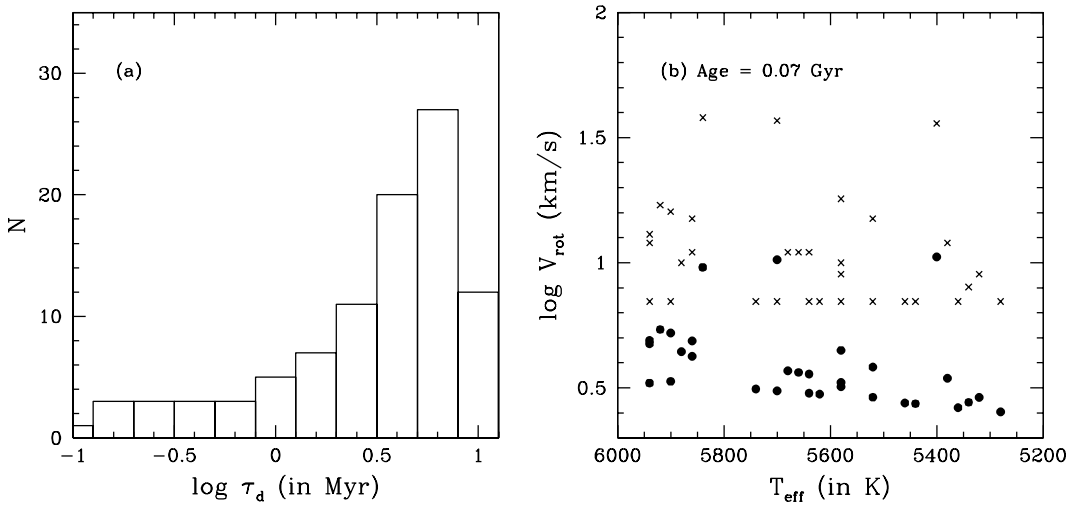

FIG. 1.—(*a*) Distribution of accretion disk lifetimes inferred from the observed rotational velocities of Pleiades stars. Data is taken from Soderblom et al. (1993a). (*b*) Measured rotational velocities of the Pleiades stars (*crosses*) in km s^{-1} and the rotational velocities of the halo composition models (*solid circles*) at an age of 70 Myr with the same T_{eff} and disk lifetimes.

A distribution of $v \sin i$ values can in principle be inverted to infer the true distribution of velocities (Chandrasekhar & Munch 1950), but the technique requires a large sample and we would lose the information on the mass dependence of rotation that is important for our purposes. Although sin i can be small, it will be close to 1 for the large majority of stars; only $\frac{1}{7}$ of the sample will have sin $i < 0.5$ for a random distribution of inclination angles. Furthermore, the young open clusters have a small population of rapid rotators and a large population of slow rotators; 13 of the 91 stars in the Pleiades sample have $v \sin i > 40$ km s^{-1}, and seven have $v \sin i$ between 20 and 40 km s^{-1}. Therefore, only a small fraction of the low–$v \sin i$ systems are intrinsically rapid rotators seen pole-on. For these reasons we have therefore chosen to apply an average statistical correction to the data and do not believe that the shape of the distribution in Figure 1 will be greatly altered by inclination angle effects. Rotation periods are not affected by sin i, and they provide an alternate means of estimating the distribution of initial conditions. Although the present rotation period samples are much smaller than the $v \sin i$ samples, the number of stars with measured rotation periods is growing, and it may soon be possible to use them in well-studied systems such as the Pleiades.

The issue of the lower envelope of rotation is a more serious concern; there is a bias in the $v \sin i$ sample against detecting truly slow rotators. We have a series of reasons for believing that the absence of very slow rotators is real. First, stellar rotation periods can be measured for stars without the uncertainty introduced by the inclination angle; much slower rotation rates can be measured with this technique than with $v \sin i$ data. Long rotation periods are not found in the Pleiades (Krishnamurthi et al. 1998) and are very rare in the T Tauri population (Edwards et al. 1993; Bouvier et al. 1993), which suggests that any population of very slow rotators is small. Furthermore, even disks that last to the main sequence would produce only stars with rotation periods of order 10 days, very close to the rotation period corresponding to the $v \sin i$ limits. We would therefore require stars that are locked to their disks with periods much longer than that seen in T Tauri stars and with long disk lifetimes to produce a population of ultraslow rotators large enough to affect our results. Finally, progressively younger open clusters have a smaller number of upper limits than older systems (there are fewer in α Per than in the Pleiades), and the lower envelope of rotation is resolved in the youngest systems (IC 2391 and IC 2602). Recent studies of rotation in the Pleiades are also consistent with this conclusion (Bouvier et al. 1997).

The universality of the distribution in Figure 1*a* is another important question. KPBS found that the distributions of disk lifetimes needed for the different young open clusters were consistent with one another, in the sense that the slow rotator distribution peaked at similar disk lifetimes for systems of different ages. This does not guarantee that the same will hold true for systems that formed under different conditions, such as halo stars and globular cluster stars. The distribution of initial rotation rates cannot be directly inferred in old systems because the surface rotation rates of stars converge as they age and lose angular momentum. Even in a system as young as the Hyades (600 Myr) the range in surface rotation rates is too small to permit a reliable estimate of the initial angular momentum of any given star. It is, however, at least a plausible starting point to ask whether or not the distribution of lithium abundances in different samples is consistent with the distribution of rotation rates seen in young open clusters such as the Pleiades. One can in principle invert the question and ask what distribution of disk lifetimes is needed to produce a given distribution of lithium abundances. Lithium depletion depends on the rotational history of a given star, and therefore the distribution of surface lithium abundances in old stars can be used to obtain information about the distribution of initial conditions in systems that are too old to provide direct information on the rotation rates. We will show that both the halo star and open cluster lithium depletion patterns are consistent with lithium depletion from rotational mixing and with being drawn from the same set of initial conditions.

3.1.2. *Metallicity Effects*

For each Pleiades star we can infer a disk lifetime; in Figure 1*b* we compare the rotation properties of halo star models with the same age, effective temperature, disk life-

time, and rotation physics (angular momentum loss law and angular momentum transport prescription). We did not run halo star models with effective temperatures as low as the bulk of the Pleiades sample, since these stars would not be on the halo lithium plateau; we have therefore shown only the $T_{\rm eff}$ range where the two samples overlap. There are some important features of this comparison that will have implications for the lithium depletion pattern in open cluster and halo stars. First, the overall level of rotation is lower in the halo stars; second, the range in rotation rates is smaller. Both phenomena can be traced to differences in stellar structure, and the relative pattern is the same as described in PDD and in Chaboyer & Demarque (1994).

At a given $T_{\rm eff}$ a halo star will have a lower total mass and moment of inertia; for the same amount of angular momentum loss the halo star will therefore spin down more rapidly. Rapid rotators lose more angular momentum than slow rotators, which causes their surface rotation rates to converge at late ages. In addition, the convergence to similar surface rotation rates occurs more quickly in the halo stars because of their smaller moments of inertia. The diffusion coefficients for mixing depend on both the absolute rotation rates and the internal angular velocity gradients; both are smaller in halo stars than in solar composition stars of the same age and $T_{\rm eff}$. The overall level of lithium depletion will therefore be lower in the halo star models. In addition, a range in surface rotation rates will produce a range in the degree of rotational mixing and therefore a dispersion in surface lithium abundances. The smaller range in surface rotation rates for the halo star models will therefore produce a smaller dispersion in surface lithium abundance at fixed $T_{\rm eff}$. Similar initial conditions will therefore produce different apparent lithium depletion patterns; this is important because such differences are clearly seen in the observational data.

There is very limited observational data on rotation rates for halo stars; this is not surprising, because the predicted level of line broadening from rotation in old stars is lower than other line-broadening sources. A $v \sin i$ limit of 8 km s^{-1} for MS halo stars was found by Peterson, Tarbell, & Carney (1983), and very high-resolution studies of a small number of halo stars find no evidence for extra line broadening above the 3—4 km s^{-1} level (Hobbs & Thorburn 1997). There is a scarcity of data for old Population I stars for similar reasons. We believe that the best means for inferring the Population II distribution of initial conditions is to develop a physical model capable of reproducing the Population I data and to then apply it to Population II models. Young moderately metal-poor open clusters may provide some clues about the impact of metal abundance on the distribution of initial conditions. Such data would provide useful additional constraints on the models; in particular, the theoretical models would predict a smaller overall range in rotation rates in a metal-poor systems than would be seen in a solar abundance system of the same age.

3.2. *Monte Carlo Simulations of Open Cluster Lithium Depletion*

Our theoretical models can be used to predict lithium depletion in open cluster and halo stars. As discussed above, the observed distribution of rotation rates in young open clusters (like the Pleiades) is mapped onto a distribution of initial rotation rates by use of an accretion disk model that, during the T Tauri phase of its pre–main-sequence evolution, locks the rotation period of the star at 10 days. A range in decoupling times for these accretion disks will then generate a range of rotation rates for stars on the main sequence as a function of time. The rotational properties of the models are calibrated on the rotational properties of the open cluster stars, and solar models are required to reproduce the solar rotation rate at the age of the Sun. This step is independent of the initial conditions for the Sun because different disk lifetimes for solar models converge to identical surface rotation rates at the age of the Sun.

We then need a means of relating the diffusion coefficients for mixing to those for angular momentum; the usual approach is to require that a solar model reproduce the solar surface lithium abundance at the age of the Sun. Because models with different disk lifetimes have different rotation histories, this step depends critically on the disk lifetime assigned to the Sun. If the Sun is assumed to have a typical rotation history then solar analogs will have lithium depletion comparable to that in the Sun. On the other hand, if the Sun was an unusually rapid rotator (i.e., had a shorter disk lifetime than most stars) the majority of other stars will have less lithium depletion. We therefore ran solar calibrated models with the Sun having disk lifetimes of 0 (anomalous), 0.3, and 1 ("typical") Myr; these cases will be referred to as s0, s0.3, and s1 for the remainder of the text. The open cluster lithium data are fit poorly when the Sun is assumed to have a disk lifetime longer than 1 Myr (see below). All of our solar disk lifetimes are shorter than the 3 Myr required for typical stars; this implies that the Sun was a faster than average rotator in its youth and thus that its rotation history was not typical, strictly speaking. The solar-calibrated models can then be used to predict the lithium depletion factor as a function of time for a given disk lifetime, mass, and composition. We then investigated the distribution of lithium depletion factors that would be produced by a given distribution of disk lifetimes. For each star we chose an initial condition at random from the Pleiades distribution of disk lifetimes; we show sample Monte Carlo runs for the four open clusters using two different solar calibrations (s0 and s1) in Figures 2 and 3, respectively. For each cluster all stars were assumed to start with the same initial lithium abundance: we chose [Li] = 3.4 for the youngest open clusters and [Li] = 3.3 for the Sun and for M67. Standard model predictions for Li in these clusters are shown as solid curves in Figures 2 and 3. Note that some main-sequence lithium depletion is demanded by the data and that the overall lithium depletion pattern as a function of age is in reasonably good agreement with the Monte Carlo simulations of the models with rotational mixing. Variations in the initial rotation rates provide a natural explanation for dispersion in stellar surface Li/H at fixed $T_{\rm eff}$.

There is a tendency for the hotter models to overdeplete lithium relative to the data in the moderate-age systems. This can be traced to the breakdown of our angular momentum loss prescription in stars close to the transition from convective to radiative envelopes. The convective overturn timescale drops rapidly with increased mass, and equation (3) therefore results in a rapid increase in the saturation threshold for angular momentum loss for the highest mass models in our simulations. These models do not reproduce the surface rotation as a function of time as well as the lower mass models do. When the saturation threshold as a function of mass is adjusted empirically to match

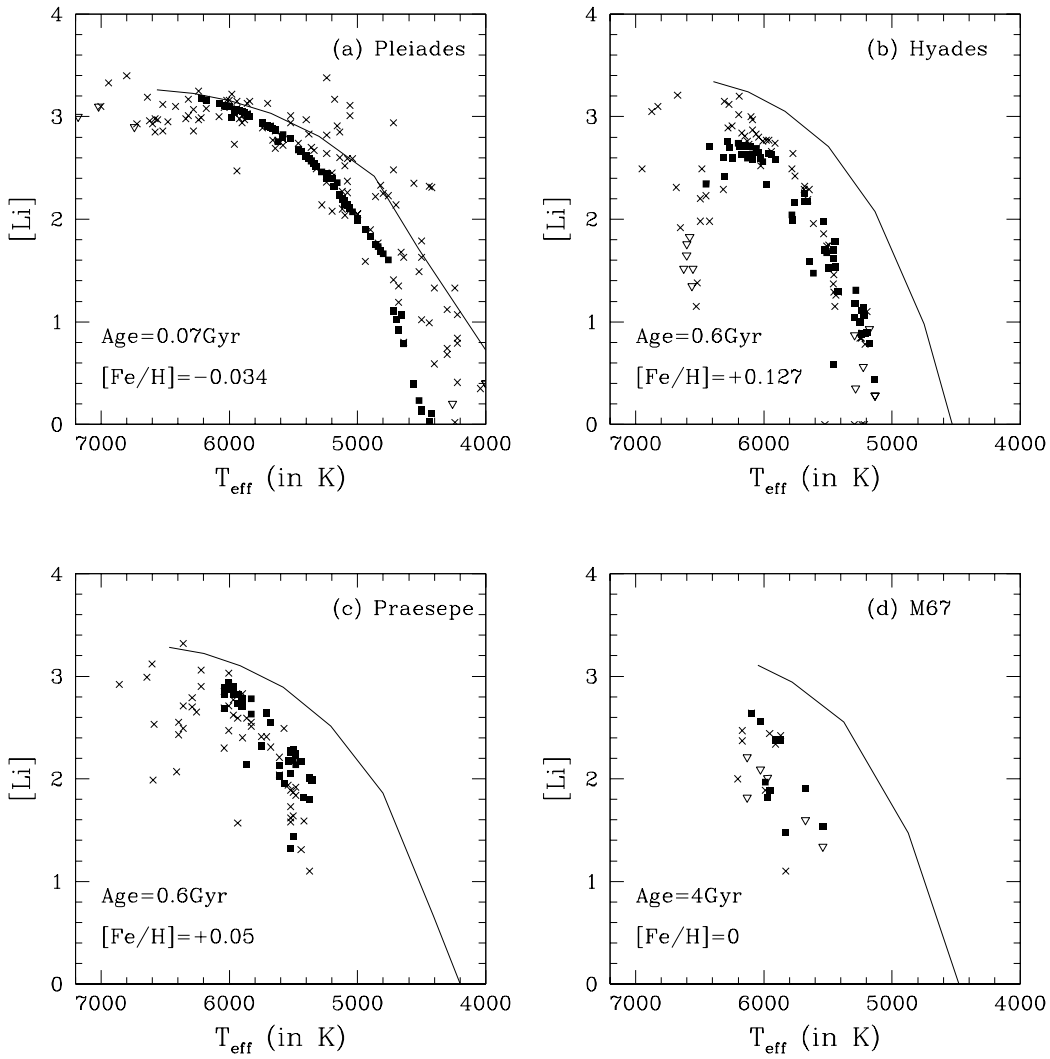

FIG. 2.—Comparison of the [Li] measured in four different open clusters (*crosses*) with the [Li] predicted by the s0 models (*filled squares*) in a typical Monte Carlo run. The open inverted triangles represent those stars for which only an upper limit is quoted in the observations. Lithium data are taken from Soderblom et al. (1993b) and Balachandran (1995). The solid lines are standard model ^{7}Li depletion factors for the metal abundances of the clusters ([Fe/H] = −0.03, +0.12, +0.04, and 0.0 for the Pleiades, Hyades, Praesepe, and M67, respectively). The initial abundance of [Li] in the theoretical models was assumed to be 3.3 for M67 and 3.4 for the other clusters.

the observed spin-down, lithium depletion in the hotter models decreases. We believe that this effect will not influence the amount of ^{7}Li depletion in our halo star models because the stars currently on the halo plateau arrived on the main sequence with a $T_{\rm eff}$ and a surface convection zone depth in the range where the current models reproduce the observed spin-down in young cluster stars. Since the angular momentum loss properties are largely set in the early phase of MS evolution, we believe that the lithium depletion pattern is also relatively well modeled (as seen in the discussion below).

The predictions of the time dependence of lithium depletion due to rotational mixing match the open cluster data best for the case in which the Sun was an unusually rapid rotator (Fig. 2). This s0 case corresponds to minimal lithium depletion and predicts modest dispersion in the open cluster lithium abundances. As the Sun is made more typical (i.e., as its disk lifetime increases and its ZAMS rotation rate drops) the overall depletion and dispersion become larger and the overall agreement with the data worsens. The intermediate-age systems are the most sensitive discriminant; the model predictions are similar in young systems and the old clusters have less data (which is also less accurate). A larger and more accurate data set for the old open cluster M67 was recently obtained by Jones, Fischer, & Soderblom (1999), and they found evidence for both a large dispersion in turnoff stars and for the Sun being overdepleted relative to solar analogues.

A more detailed analysis of the open cluster lithium depletion pattern will be presented in a paper in preparation (Narayanan et al. 1999); for the purposes of this paper, we note that open cluster models constructed using the same technique that we have applied to halo stars are in overall agreement with the observed lithium depletion pattern.

3.3. *Halo Stars*

3.3.1. *Parameter Variations*

We can extend the Pinsonneault, Narayanan, & Krishnamurthi (1996) models, designed for rotational mixing in open clusters, to study lithium depletion in halo stars. Unlike the open clusters, the halo stars have a range in

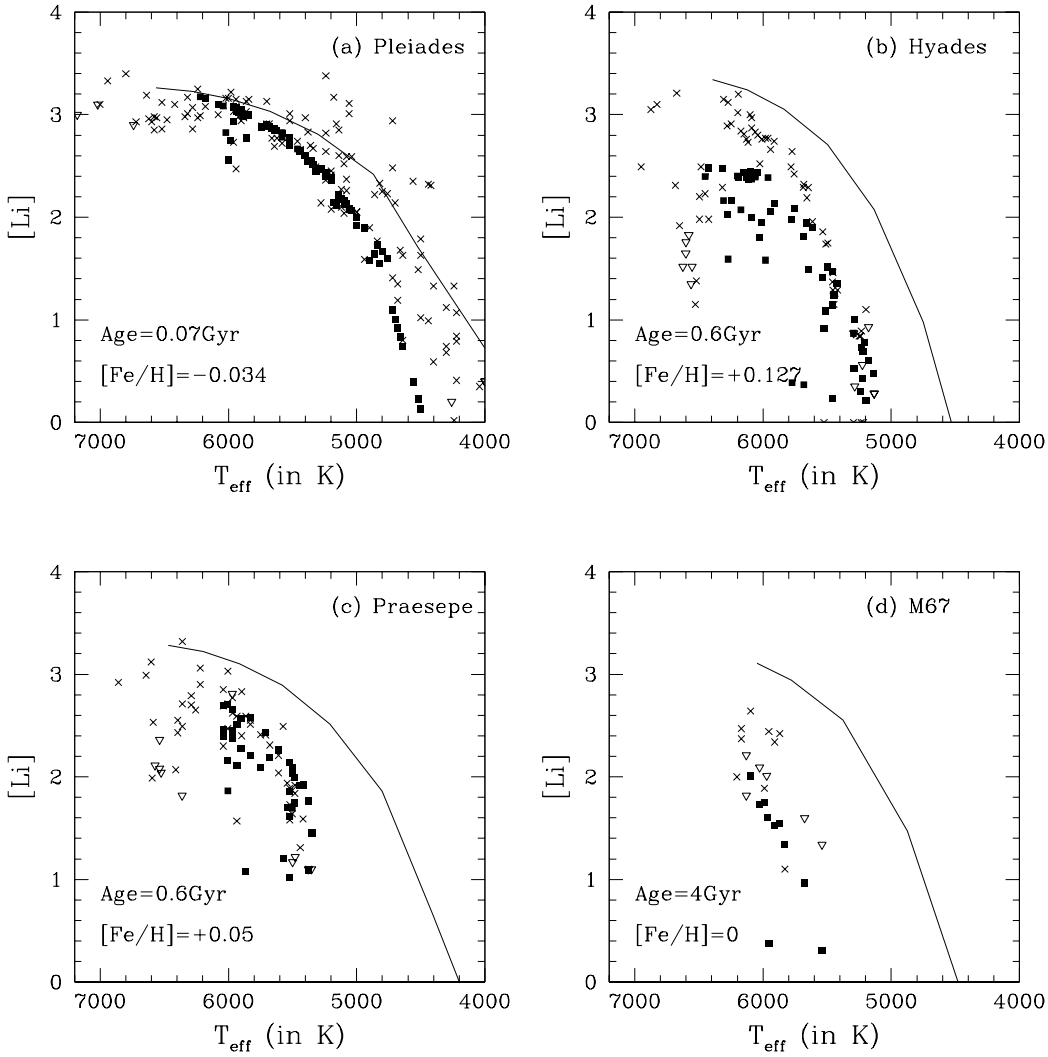

FIG. 3.—As Fig. 2, except for a Monte Carlo simulation using the s1 case

metal abundance and age. We therefore begin with a discussion of the dependence of the lithium depletion pattern on the important components of our models: disk lifetimes, solar calibration, metal abundance, and age. In Figure 4 we show the effects of changes in all of these ingredients. In all panels the solid line is a base case that corresponds to models with a 3 Myr disk lifetime, [Fe/H] = −2.3, and an age of 12 Gyr.

3.3.1.1. Disk Lifetime

A range in disk lifetime can produce significant variations in the predicted lithium depletion, especially for the rapid rotators. This will manifest itself as a dispersion in lithium abundance at fixed $T_{\rm eff}$ (Fig. 4*a*). However, the large majority of stars in the Pleiades are slow rotators with disk lifetimes greater than 1 Myr. As we will see below, the intrinsic range in depletion factors for slow rotators is very small; i.e., only the top 20% of the distribution will have depletion factors greater than or equal to the depletion factor of the 1 Myr case (see Fig. 1*a*), while the remainder will have depletion factors similar to that for the 3 Myr case. The overall pattern that would be expected from the Pleiades distribution of initial conditions is therefore a majority of stars with a small intrinsic range in abundance with a subpopulation (corresponding to rapid rotators) that is overdepleted with respect to the bulk of the stars.

3.3.1.2. Solar Calibration

The solar calibration sets the overall level of depletion in the models, and it will therefore have a strong influence on the derived primordial lithium abundance (Fig. 4*b*). Once the solar calibration is set by the open cluster data, it should be the same for all stars (Chaboyer & Zahn 1992), and in particular for halo stars. That is, we expect that the best fit to the halo star lithium abundances will correspond to the limit in which the Sun is overdepleted in lithium relative to its counterparts (the s0 case).

We define the depletion factor D_7 as the ratio of the initial (^{7}Li/H) to the current surface (^{7}Li/H). The halo star models of PDD predicted a value of D_7 close to 10 for plateau stars, with little dependence on the model parameters. This behavior is very different from that illustrated in Figure 4, and this can be traced to differences in the initial conditions and angular momentum loss law. PDD began with a modest range of initial angular momenta (a factor of 10) and applied a loss law that caused a rapid convergence in the surface rotation rates. We begin with a wider range of initial angular momenta (disk lifetimes from 0 to 10 Myr

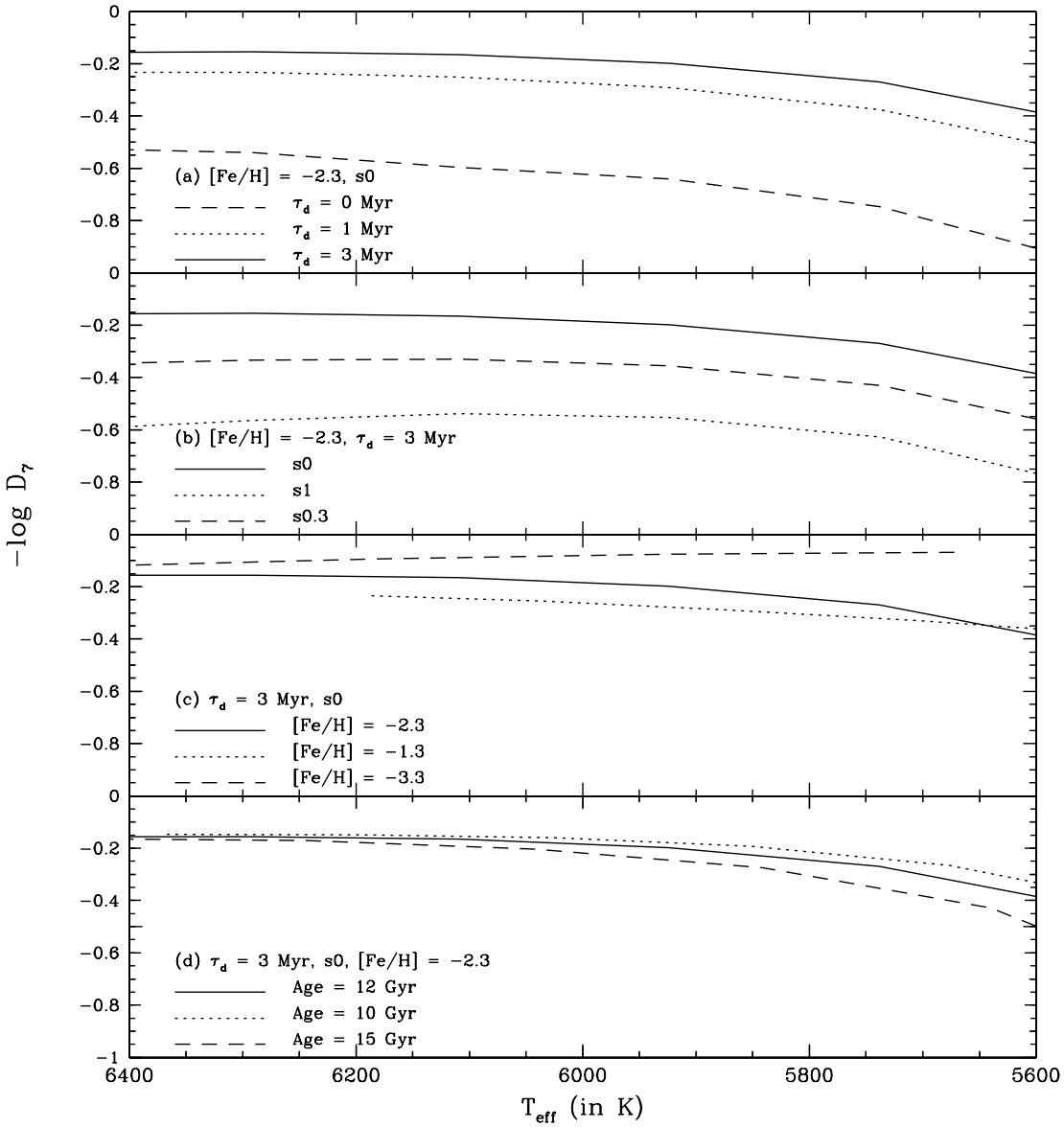

FIG. 4.—Sensitivity of the lithium depletion patterns to changes in (*a*) the timescale for coupling between the accretion disk and the protostar in Myr (τ_d), (*b*) the solar calibration (accretion disk lifetime for the Sun), (*c*) [Fe/H], and (*d*) age. In all these panels, the solid line represents a base case for a typical halo star with $\tau_d = 3$ Myr, [Fe/H] $= -2.3$, s0 and age $= 12$ Gyr. D_7 is defined as the ratio of the current surface ^{7}Li to the initial ^{7}Li.

will produce a factor of 16 range in angular momentum at an age of 10 Myr). The loss law that is required by the rotation data also permits a wide range of rotation rates to persist for a longer period of time than it did in the models of PDD. The net result is a much larger possible range of lithium depletion factors. The models of PDD, for example, had a total range in log D_7 of 0.25 dex at 0.7 $M_\odot$ and [Fe/H] $= -2.3$, while the corresponding models in the current study have a range in depletion factors of 0.50 dex (s0) to 1.30 dex (s1). Because the possible range of lithium depletion factors is greatly increased, the choice of the initial conditions for the Sun becomes correspondingly more important. In effect, the earlier generation of models had a small enough effective range in initial conditions that the Sun was by definition a typical star, and the typical depletion factors were therefore forced to be similar to those for the Sun. If the Sun is treated as a typical star with a disk lifetime of 3 Myr, we recover the mean depletion factor of PDD log $D_7 = -1.0$) with a much larger range of depletion factors than permitted by the data.

3.3.1.3. Metal Abundance

Models with different metal abundance differ in their overall lithium depletion factors by a modest amount, less than 0.1 dex change in lithium depletion per 1.0 dex change in [Fe/H]. The overall trend is in the sense that the more metal-rich stars deplete more than the more metal-poor stars; this is to be expected in light of the relative differences between solar composition and halo star rotational properties illustrated in Figure 1.

This is opposite to the trend found by Thorburn (1994) in the observational data, for which stars with lower metal abundance have, on average, slightly lower lithium abundances, by 0.1 dex in [Li] for 1.0 dex in [Fe/H]. However, there are some possible complications in this relative comparison. The slope of the [Li]-[Fe/H] relationship depends

upon the assumed model atmospheres. Furthermore, the derived value of the slope depends on the data analysis method that is used and is different for different subsets of the data (Ryan et al. 1996). By contrast, the [Li]-$T_{\rm eff}$ slope reported by Ryan et al. (1996) is resistant to these effects.

Within the framework of the rotational mixing hypothesis, one would also expect stochastic variations in the disk lifetimes and therefore an additional random component in the lithium abundances. Since about 20% of the Pleiades stars have modest to rapid rotation, the sample could (for example) happen to have slightly more rapid rotators at low [Fe/H] and slightly fewer at relatively high [Fe/H] by chance; this effect is not included in the Ryan et al. (1996) or Thorburn (1994) analysis.

Another possibility is that the trends in the models and the data are correct, and that Galactic production of ^{7}Li is responsible for the difference between the trends. In all of the models we require some lithium production during the lifetime of the Galaxy; this would imply that the more metal-rich stars begin with slightly more lithium, which would counteract the [Li]-$T_{\rm eff}$ trend predicted by the models. The Galactic evolution of lithium remains a mystery, but we can estimate the effect as follows. If we scale the solar system lithium abundance ([Li] = 3.3) linearly with metallicity, the newly produced lithium will contribute Δ[Li] = 0.0, 1.0, and 2.0 at [Fe/H] = -3.3, -2.3, and -1.3, respectively. Note that if the post-BBN lithium production scales faster than linearly with metallicity such halo contamination will be negligible. We infer a primordial abundance in the range [Li] = 2.35–2.75. The total abundance at the low end of the range (primordial plus production) would therefore be 2.35, 2.37, and 2.51 at [Fe/H] = -3.3, -2.3, and -1.3, respectively; by comparison, at the high end of the range the comparable abundances would be 2.75, 2.76, and 2.82. This suggests that Galactic production could influence the Li-[Fe/H] slope at higher metal abundances but not for abundances below -2.3.

As we will show below, the detection of ^{6}Li in HD 84937 requires some ^{6}Li and ^{7}Li production at early epochs; this production could have been highly variable and possibly even largely absent for the most metal poor stars. We therefore cannot exclude an additional production component between the very metal-poor stars and the more typical plateau stars, but we caution that there may not be a reliable relationship between production and metal abundance in this case. If the level of ^{6}Li seen in HD 84937 is typical for stars at [Fe/H] = -2.3, and the production of ^{7}Li by α-α fusion is comparable to that of ^{6}Li, then we can set an upper limit on the variation in the initial ^{7}Li abundance between the most metal-poor stars and the typical plateau stars by computing the ^{7}Li yield required to produce the observed ^{6}Li in HD 84937. The ^{7}Li yield required to explain the observed ^{6}Li in HD 84937 is in the range $3–7 \times 10^{-11}$. This suggests that variable production of ^{7}Li could have a modest impact on the [Li]-[Fe/H] slope even at early epochs.

In light of the uncertainties discussed above, we have adopted an empirical approach. The value of the [Li]-[Fe/H] slope that minimizes the dispersion in the data set is computed, and the observed lithium abundances are then corrected for the effects of metallicity. We have therefore used the [Fe/H] = -2.3 models for our theoretical calculations and corrected the Thorburn (1994) abundances to a uniform [Fe/H] at this level using the relationship of Thorburn (1994),

$$[\mathrm{Li}]_{\rm detrended} = [\mathrm{Li}]_{\rm observed} + 0.13([\mathrm{Fe/H}] + 2.3) . \quad (4)$$

This raw data is compared with the data corrected to a uniform abundance of -2.3 in Figure 5. We note that another approach would be to draw the distribution of theoretical depletion factors from the distribution of [Fe/H] in the Thorburn sample, i.e., to Monte Carlo both the initial conditions and the [Fe/H] abundances. In numerical tests the correction in equation (4) reduces the dispersion in the data set by an amount comparable to the level introduced by the observed distribution of metal abundances convolved with the theoretical models.

3.3.1.4. Age

The final ingredient is age; as shown in Figure 4*d* even significant variations in age produce only small changes in the lithium abundance at fixed $T_{\rm eff}$. This results from a combination of a low rate of lithium depletion at old ages and the evolutionary changes in $T_{\rm eff}$ as a function of time, which move models along the plateau. We therefore neglect the impact of age variations on the dispersion and depletion patterns.

3.3.2. *Monte Carlo Simulations: Trends with $T_{\rm eff}$ and Dispersion*

Monte Carlo simulations of the lithium abundances of halo stars are compared with the Thorburn (1994) data set detrended to a uniform [Fe/H] of -2.3 in Figure 6. The different models all show a [Li]-$T_{\rm eff}$ trend similar to the data. Previous models with rotational mixing had a downward curvature at the hot end of the plateau, which is highly suppressed in these models, although there is a slight downward curvature in the s1 case. This difference can be attributed to improvements in the angular momentum loss law. The open cluster rotation data requires stronger angular momentum loss for higher mass stars. Higher mass models therefore arrive on the main sequence with lower total angular momentum relative to lower mass models than they did in earlier calculations. Because the level of MS angular momentum largely determines the degree of mixing, this

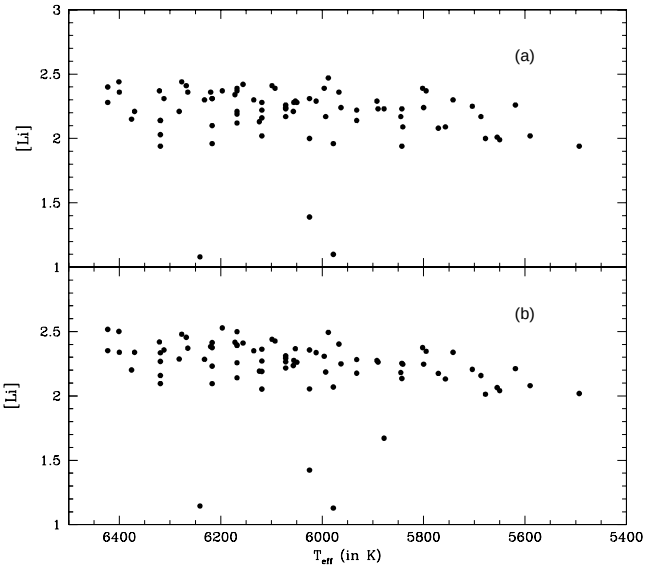

FIG. 5.—[Li] in halo stars (*a*) before and (*b*) after correcting for the metallicity trends. The abundance data were taken from Thorburn (1994) and corrected to a uniform metal abundance using eq. (4).

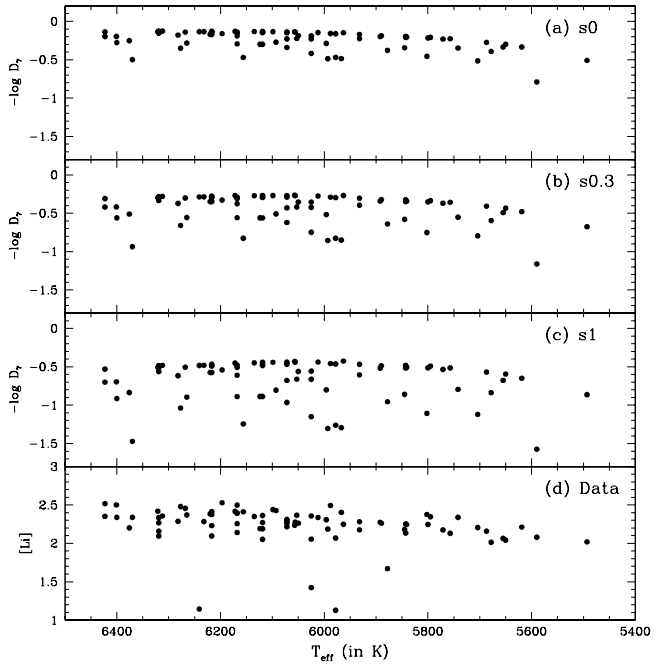

FIG. 6.—Sample Monte Carlo distributions of ^{7}Li depletion factors for the three different solar calibrations: (*a*) s0, (*b*) s0.3, and (*c*) s1. (*d*) Thorburn (1994) lithium data corrected to a uniform metallicity of [Fe/H] = −2.3.

acts to preferentially suppress lithium depletion in the higher mass models at the hot end of the plateau relative to models for cooler lower mass stars.

The Pleiades distribution of initial conditions also produces a mean trend with small internal scatter and a smaller population of overdepleted stars. As the solar disk lifetime is increased, the dispersion and overall depletion both increase; we can therefore use the dispersion in the halo plateau to set constraints on the overall depletion. The simulations in this section do not include observational errors, whose impact on dispersion estimates will be discussed in the next section. The Thorburn sample also contains a small population of highly overdepleted stars; their existence is a problem for standard stellar models, and they are usually ignored in discussions of the dispersion in the halo plateau. We will not ignore the outliers; in fact, such objects are a natural consequence of the models with rotational mixing combined with the observed distribution of rotation rates in young clusters. The maximum depletion level for the rapid rotators also increases as the absolute depletion increases. The existence of highly overdepleted stars can therefore be used to constrain the minimum level of absolute depletion in the halo plateau; if the absolute depletion in the halo plateau is too small then stars far below the plateau should not be present, but they are.

Both the trends in the [Li]-$T_{\rm eff}$ plane and the dispersion in the plateau have been used to argue against significant lithium depletion in halo stars. The simulations in Figure 6 indicate that the current class of models are compatible with both, but the agreement between the data and the models worsens if the absolute depletion is too high. Similar trends are present in the open cluster simulations. *In other words, the open cluster and halo star data are consistent with being drawn from a ZAMS angular momenta distribution similar to that required to explain the distribution of rotation rates in young open clusters. Furthermore, both are best explained by a solar calibration in which the Sun had an accretion disk lifetime shorter than the typical value for low-mass stars.*

In the next section we quantify the constraints placed on the overall lithium depletion by the dispersion and the highly overdepleted stars. We also discuss the relative lithium 6 and lithium 7 depletion factors and constraints on the overall destruction of lithium 7 from the detection of lithium 6 in HD 84937.

4. CONSTRAINTS ON ROTATIONAL MIXING FROM HALO STARS

4.1. *Dispersion of the Plateau Abundances*

Lithium abundances versus effective temperatures for warm ($T_{\rm eff} \gtrsim 5800$ K), metal-poor ([Fe/H] ≤ -1.3) stars (as observed by Thorburn 1994) were shown in Figure 5. Four independent groups have observed Population II plateau stars (Spite & Spite 1982; Spite, Maillard, & Spite 1984; Rebolo, Molaro, & Beckman 1988; Thorburn 1994). The differences in the lithium abundances derived by different observers from Population II halo stars can be traced to the choice of temperature scale and of model atmosphere required to extract an abundance from an observed absorption line. A survey of the literature shows that there may be a systematic uncertainty in the lithium abundance scale of order ± 0.1 dex because of the choice of atmosphere model and of the stellar temperature scale. The intrinsic star-to-star dispersion is likely to be much smaller than this. There may also be correlations in the data in the sense that the lithium abundance increases slightly with effective temperature and with metallicity (Thorburn 1994; Ryan et al. 1996) or not (Molaro et al. 1995). We adopt $[{\rm Li}]_{\rm PopII} = 2.25 \pm 0.10$ as the weighted mean plus estimated systematic error of all the plateau data. The raw dispersion about the trend is 0.16 dex (Thorburn 1994). When the $T_{\rm eff}$ and [Fe/H] trends are removed, Thorburn estimated the dispersion as 0.13 dex; by comparison, her estimate of the observational error is 0.09 dex. Estimates of the intrinsic star-to-star dispersion are therefore roughly one-half the raw dispersion (0.08 dex: Deliyannis, Pinsonneault, & Duncan 1993; 0.06 dex: Thorburn 1994; <0.1 dex:Bonifacio & Molaro 1997).

In our rotationally mixed models, the "anomalous Sun" case corresponds to lithium depletion of 0.2 dex and a dispersion in depletion of 0.09 dex, consistent with estimates of the intrinsic dispersion. The intermediate disk case corresponds to lithium depletion of 0.4 dex and a dispersion in depletion of 0.16 dex, which is at the limit of the raw dispersion. The "typical Sun" case corresponds to lithium depletion of 0.69 dex and a dispersion of 0.25 dex, which is considerably larger than the raw dispersion. This initial comparison suggests that an upper bound to lithium depletion in halo stars is 0.4 dex. If the Sun is anomalous (as favored by the open cluster data) then little dispersion in the plateau is predicted, consistent with the data, along with a smaller overall depletion of 0.2 dex. Therefore, two indicators, the open cluster data along with the lack of significant dispersion in the halo lithium abundances, both point to halo star lithium depletion in the range 0.2–0.4 dex.

We have chosen to use the Thorburn (1994) sample. It is the largest and most uniform data set, with 73 plateau stars, as compared with 41 plateau stars in the Bonifacio & Molaro (1997) sample; in addition, it includes a larger number of more metal-poor stars than the Bonifacio &

Molaro (1997) sample. There is one highly overdepleted star in the Bonifacio & Molaro (1997) sample, roughly comparable to the fraction in the Thorburn sample. The overall dispersion in the Bonifacio & Molaro (1997) is smaller than in the Thorburn sample—0.094 dex excluding the outlier—with an estimated error of 0.083 dex. However, the temperature errors in the method used by Bonifacio & Molaro (1997) include both random and systematic sources. Typical random temperature errors for photometric indices are at the 50 K level. If a uniform error of 50 K is assumed, the dispersion expected from the errors drops to 0.06 dex and an intrinsic component of 0.07 dex is implied. For our purposes, the Bonifacio & Molaro (1997) data set would therefore favor the lower end of our depletion range, i.e., 0.2 dex.

However, the calculation of the observational dispersion excludes six upper limits, and the distribution of theoretical depletion factors is significantly non-Gaussian. We can use these additional characteristics of the plateau data to constrain the absolute depletion. Standard models would require that the only dispersion in halo star lithium abundances is due to age, metal abundance, and observational error. Age is a small effect in all classes of models, and the effects of metal abundance can be included by detrending the data. We would therefore expect the shape of the distribution to be determined by the observational errors and thus it should be Gaussian.

By contrast, the distribution of lithium depletion factors in rotational models is skewed. The majority of young cluster stars are slow rotators, so the majority of the depletion factors are tightly clustered with a very small intrinsic dispersion; there is a component of stars with moderate rotation rates that produce a population with larger depletion factors and a small fraction (2%–3%) of rapid rotators with large depletion factors. In addition, the distribution will be smeared out by observational errors. We ran 1000 Monte Carlo simulations at intervals of 50 K across the plateau and drew theoretical lithium depletion factors from the Pleiades distribution of initial conditions. In one set of runs, observational errors were neglected; in a second set of runs we added a random error of 0.09 dex. The lithium depletion factors for each $T_{\rm eff}$ were then sorted. In Figure 7 we compare the detrended Thorburn data (Fig. 7*c*) with the 2.5%, median, and 97.5% bounds of the theoretical depletion factors for our s0 case (Fig. 7*a*), s0.3 case (Fig. 7*b*), and s1 case (Fig. 7*c*). The zero point was set by requiring that one-half the stars in the sample for all three cases were above the median and one-half the stars were below it. Figure 8 presents the same cases for simulations that include observational errors. The top and bottom dashed lines can be regarded as effective $\pm 2\ \sigma$ bounds. *Note that the observed lithium abundances have a similar morphology to the simulations; in particular, they are not Gaussian distributed about the mean as would be expected if these stars had suffered no lithium depletion.* Furthermore, the intrinsic dispersion for the majority of stars is significantly less than the observational errors; in other words, the dispersion for the majority of stars is dominated by observational errors. The theoretical models predict that there should be a small number of highly overdepleted stars, which are indeed observed.

This can be further quantified by comparing the distribution of abundances about the median for the simulations to the observed distribution of abundances about the median. We chose a reference temperature of 6000 K and an [Fe/H]

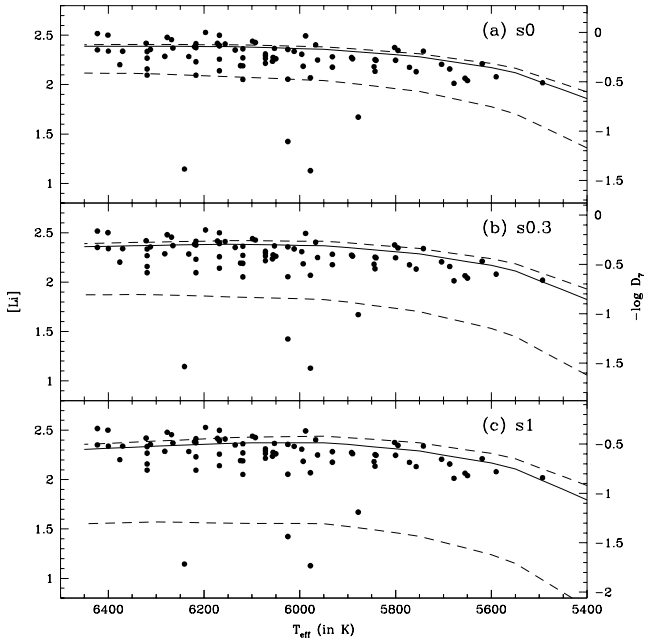

FIG. 7.—Lithium depletion factors for the three different solar calibrations before accounting for the observational errors: (*a*) s0, (*b*) s0.3, and (*c*) s1. The solid line shows the median value, while the dashed lines show the 2.5 and 97.5 percentile values. The filled circles show the observed [Li] in the halo stars after correcting them all to the same metallicity of [Fe/H] = −2.3.

of −2.3 for the simulations and used the Thorburn (1994) mean trend to correct the data to a uniform $T_{\rm eff}$ and [Fe/H]. Histogram plots of the number of stars as a function of lithium abundance are compared to the number of stars as a function of lithium depletion factor expected in the simulations without and with observational errors in Figures 9 and 10, respectively. The s0 case is a good match to the width of the distribution, while the s0.3 case is in marginal agreement, and the s1 case clearly has a dispersion too large to be compatible with the data. For comparison

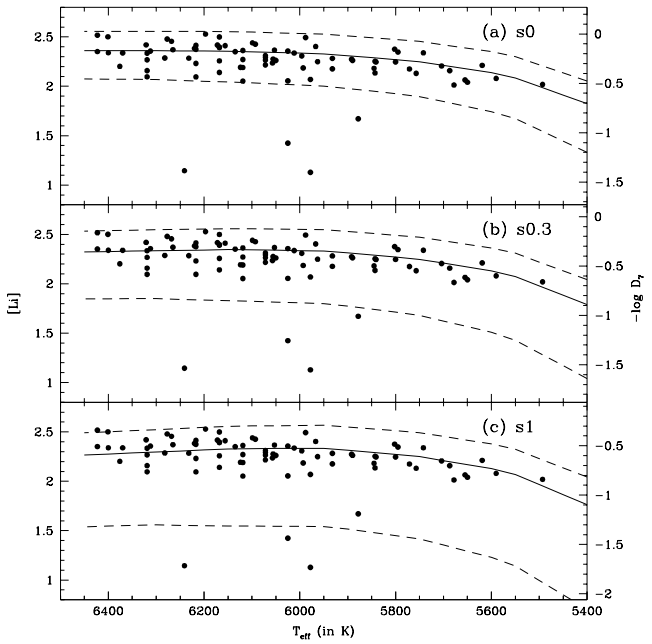

FIG. 8.—As Fig. 7, except a random observational error of 0.09 dex was included in the theoretical simulations.

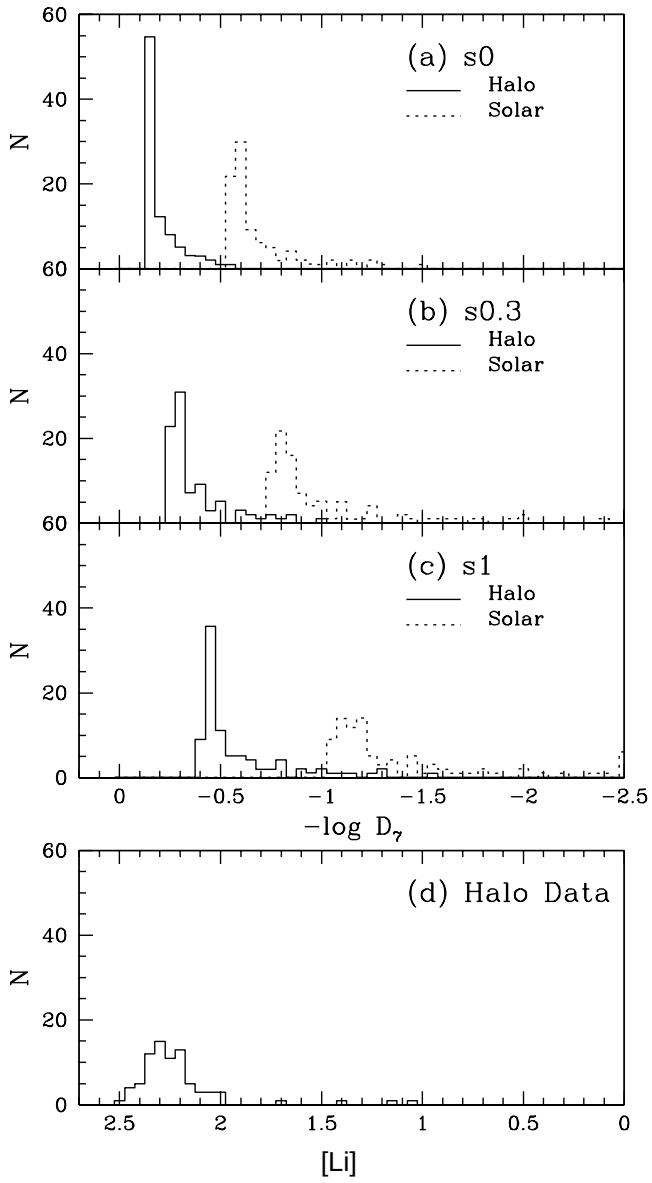

FIG. 9.—Distribution of the lithium depletion factors for the three different solar calibrations before accounting for the observational errors. All the depletion factors are estimated at $T_{\rm eff} = 6000$ K and [Fe/H] = −2.3. The top three panels show the results for the three different solar calibrations: (*a*) s0, (*b*) s0.3, and (*c*) s1. The dashed histograms are the distributions of depletion factors for the same $T_{\rm eff}$ of 6000 K but with a solar [Fe/H]. (*d*) Observed distribution of [Li] in the halo stars after correcting them all to a metallicity of [Fe/H] = −2.3. A correction of 0.04 ($T_{\rm eff}$ − 6000 K) was also applied to the data to correct for the dependence of [Li] on effective temperature.

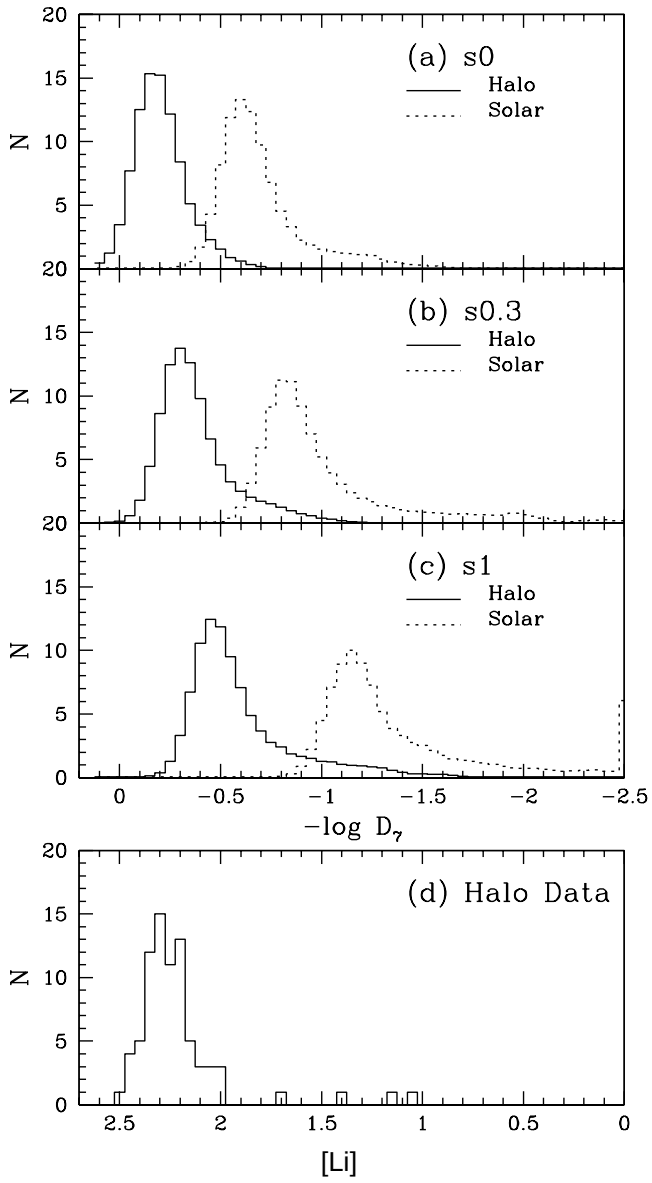

FIG. 10.—As Fig. 9, except a random observational error of 0.09 dex was included in the simulations.

purposes, an analogous distribution of depletion factors for solar abundance models at a temperature of 6000 K is also shown.

The dispersion in the bulk of the halo population is therefore consistent with overall depletions in the range of 0.2–0.4 dex, with lower depletion factors being favored. However, the existence of highly overdepleted stars can also be used to set bounds on the absolute depletion, and this favors higher absolute depletion factors in the above range. For the s0 case, the median depletion is 0.2 dex and the maximum is 0.6 dex; stars more than 0.4 dex below the plateau should therefore not be seen, in contradiction with the data. The corresponding bounds for the s0.3 case are 0.4 and 1.2 dex, permitting stars as much as 0.8 dex below the plateau; this is in better agreement with the data. We also note that the observed fraction of such stars (4 of 90) is similar to the fraction of very rapid rotators in young open clusters. We therefore conclude that the distribution of lithium abundances in the plateau is consistent with a range of 0.2–0.4 dex absolute depletion, with the bulk dispersion favoring lower values and the overdepleted stars favoring higher values within this range.

4.2. ^{6}Li *Depletion*

In Figure 11 we show the relationship between ^{7}Li destruction and ^{6}Li destruction in the rotationally mixed models chosen to correspond to the hot halo subgiant HD 84937 ([Fe/H] ≈ −2.2 and ^{6}Li/^{7}Li ≈ 0.06) (Smith, Lambert, & Nissen 1993; Hobbs & Thorburn 1994,1997), to date the only star in which the detection of ^{6}Li has been confirmed by more than one group (see Hobbs & Thorburn 1997 for a detailed observational summary of the ^{6}Li data). Note that, depending on the solar normalization, the ratio

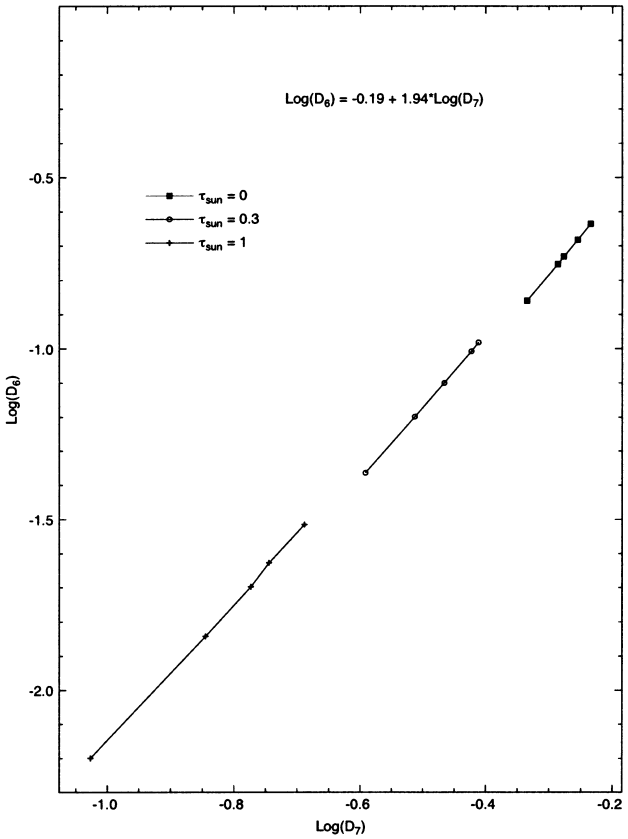

FIG. 11.—^{6}Li depletion as a function of ^{7}Li depletion for models of HD 84937. Three different solar calibrations are shown. For each calibration the ^{6}Li and ^{7}Li depletion factors are indicated by the symbols (*squares*, *open circles*, and *crosses*) for disk lifetimes of 1, 2, 3, 5, and 7 Myr (running from lower left to upper right, respectively). We have connected these discrete points by solid lines in each case. A least-squares fit to ^{6}Li depletion as a function of ^{7}Li depletion for a disk lifetime of 3 Myr is also indicated.

of ^{6}Li destruction to ^{7}Li destruction can vary from a few (for the s0 case) to 10 (for the s1 case). The absolute ^{6}Li depletion factor varies between roughly 6 and 70, respectively. Note that this is not the usual folklore of lithium depletion, which anticipates substantial ^{6}Li destruction in any star where even minimal ^{7}Li destruction has occurred (Brown & Schramm 1988; Vauclair & Charbonnel 1998). Indeed, it has often been argued that because ^{6}Li has been observed in at least one halo star, there can be little, if any, ^{7}Li depletion in any Population II plateau stars (Steigman et al. 1993). However, this argument was based on standard models without rotational mixing, in which all the lithium destruction is by convective burning during the star's approach to the main sequence. Then, since ^{6}Li is much more fragile than ^{7}Li, any star in which ^{6}Li is not significantly destroyed is not expected to destroy any ^{7}Li at all. This ^{6}Li-^{7}Li connection is relaxed in models that include rotational mixing. In the convective burning only models, all the material on the surface has been exposed to the same temperature whereas in models with rotational mixing different fractions of the surface material are exposed to different temperatures. Although the rank ordering (with binding energy) of the magnitude of lithium destruction is preserved (i.e., ^{6}Li is always destroyed more than ^{7}Li), the relative amounts of depletion can vary since the surface of the star is a mixture of gas that has been exposed to different temperatures. Note also that rotational models predict a dispersion of ^{6}Li depletion at fixed $T_{\rm eff}$ corresponding to different initial rotational velocities as drawn from a distribution of initial conditions. Below we use the Population II ^{6}Li observations to further constrain models of rotational mixing and overall lithium depletion.

To use the observed abundance of ^{6}Li as a constraint on the amount of lithium depletion, we require an estimate of its initial abundance. ^{6}Li is produced in interesting (i.e., observable) amounts by cosmic-ray nucleosynthesis via only two channels: (1) cosmic-ray proton and α spallation of CNO nuclei in the ambient ISM (and vice versa) and (2) α-α fusion reactions. To avoid introducing more adjustable parameters than can be constrained by the observational data, we can tie the CNO contribution of ^{6}Li to the observed abundances of B and Be, which are produced by the same spallation process. The Be and B abundances in Population II halo stars are observed to increase linearly with Fe/H (Duncan et al. 1997), and, therefore, so too should the "CNO-tagged" ^{6}Li. The predicted ratio of spallation-produced ^{6}Li to Be or B depends on the specific cosmic-ray spectrum and relative target/projectile abundances adopted. Some of these details can be avoided if we simply normalize ^{6}Li production to the solar abundance of ^{6}Li ($[^6{\rm Li}]_\odot \sim 2.2$): $[^6{\rm Li}]_{\rm CR(CNO)} = [^6{\rm Li}]_\odot + [{\rm Fe/H}] = 2.2 + [{\rm Fe/H}]$. This represents an upper limit to the CNO cosmic-ray (CR) production of ^{6}Li at any epoch. Since the metallicity of the Spite plateau stars is $[{\rm Fe/H}] \leq -1.3$, the CNO contribution will, in general, be quite small: $[^6{\rm Li}]_{\rm CR(CNO)} \leq 0.9$. If this were the only production mechanism for ^{6}Li in halo stars, it would, along with the plateau value of [Li] $\sim$ 2.2, correspond to a ratio $^6{\rm Li}/^7{\rm Li} \leq 1/20$, which is comparable to that observed. In this case (production via spallation of CNO) there would be room for little, if any, ^{6}Li destruction.

To quantify this point, consider the case of HD 84937, a hot ($T_{\rm eff} \sim 6300$ K) metal-poor star in which ^{6}Li observations have been claimed by two independent groups (Smith et al. 1993; Hobbs & Thorburn 1994, 1997). They find $[{\rm Fe/H}] = -2.2 \pm 0.2$ and $[^6{\rm Li}]_{\rm OBS} = 1.0^{+0.1}_{-0.2}$, an order of magnitude more ^{6}Li than the maximum predicted from CNO spallation alone: $[^6{\rm Li}]_{\rm CR(CNO)} = 0.0 \pm 0.2$. It must be emphasized that this can NOT be used as evidence for the absence of ^{6}Li destruction in halo stars but instead points to the necessity of an additional source for the observed ^{6}Li (in particular, one that does not scale with metallicity).

Alpha-alpha fusion synthesis of ^{6}Li (Steigman & Walker 1992, hereafter SW) is not necessarily coupled to the cosmic-ray spallation production of Be and B and could, in principle, be such a source of ^{6}Li (and a comparable amount of ^{7}Li). Naively we expect the fusion contribution to scale as one lower power of Fe/H than does the CNO-spallation contribution (i.e., that it may be nearly independent of metallicity). As before for spallation, the normalization of the α-α ^{6}Li contribution is essentially arbitrary. As an extreme upper limit to the abundance of α-α produced ^{6}Li in the gas out of which the Population II stars form, we may adopt the solar abundance:

$$[^6{\rm Li}]_{\rm CR(\alpha\alpha)} \leq 2.2 \, . \qquad (5)$$

This bound is certainly robust (and most likely overly conservative) since it assumes that CR fusion in the very early Galaxy generated ^{6}Li at the solar abundance. Nevertheless, it represents the maximum amount of ^{6}Li any Population II star could contain. Defining the ^{6}Li depletion

factor, D_6, as $(^6\mathrm{Li/H})_{\mathrm{OBS}} \equiv (^6\mathrm{Li/H})_{\mathrm{CR}(\alpha\alpha)}/D_6$, we have for HD 84937

$$\log D_6 < 1.2^{+0.2}_{-0.1} . \quad (6)$$

That is, there is a model-independent upper bound to ^{6}Li destruction of a factor of 14–25 for HD 84937. The rotational models for HD 84937 that violate this constraint (i.e., destroy too much ^{6}Li) are the same ones that generate too much dispersion in the plateau abundance of ^{7}Li and do not correctly predict the behavior of the lithium abundances in open clusters. This D_6 constraint allows us to obtain an independent upper bound on the depletion of ^{7}Li in Population II plateau stars (see Fig. 11) of 0.5–0.6 dex. We comment here that, although Lemoine et al. (1997) claim to have constrained D_6 to be strictly less than 4, they did not include the fusion production of ^{6}Li via α-α, which we have seen may be required if ^{6}Li has been detected in HD 84937.

4.3. *Relative Depletion of* ^{6}Li *and* ^{7}Li

Since post-BBN production of lithium can compete with surface depletion, lithium production and destruction are coupled. Thus the dispersion in the Population II lithium data itself can be used to bound any contributions to the observed Population II lithium abundance from post–big bang production and/or stellar destruction. Every Population II star should start with the same amount of BBN-produced ^{7}Li, and variations in post-BBN production and stellar destruction will contribute to dispersion in the observed "plateau" abundances. Any observational limits to the dispersion provide a limit to the combination of CR production and stellar depletion of lithium in the halo stars. That is, for any halo star, the observed total (^{7}Li plus ^{6}Li) lithium abundance can be expressed as

$$y_{\mathrm{Li}}^{\mathrm{OBS}} = \frac{y_{7\mathrm{BBN}} + y_{7\mathrm{CR}}}{D_7} + \frac{y_{6\mathrm{CR}}}{D_6} , \quad (7)$$

where the various y_7's represent the observed (OBS), BBN, and cosmic-ray–produced (subscript "CR") number fractions of ^{7}Li relative to hydrogen. The CR contribution to the observed lithium, with account taken of stellar depletion, may be bounded by the dispersion in the observed lithium abundances:

$$\frac{y_{7\mathrm{CR}}}{D_7} + \frac{y_{6\mathrm{CR}}}{D_6} \leq \Delta y_{\mathrm{Li}}^{\mathrm{OBS}} \approx 0.8 \times 10^{-10} , \quad (8)$$

where we have assumed that the BBN contribution is fixed by the minimum of the plateau:

$$\frac{y_{7\mathrm{BBN}}}{D_7} = (y_{\mathrm{Li}}^{\mathrm{OBS}})_{\mathrm{min}} \approx 1.4 \times 10^{-10} . \quad (9)$$

To bound D_6/D_7 we may then write for the (inverse of the) ^{6}Li fraction

$$\left(\frac{\mathrm{Li}}{^6\mathrm{Li}}\right)_{\mathrm{OBS}} = \frac{D_6}{D_7}\left(\frac{y_7}{y_6}\right)_{\mathrm{CR}}\left[\frac{y_{7\mathrm{BBN}}}{y_{7\mathrm{CR}}} + 1\right] + 1 . \quad (10)$$

These relations can be used along with the observational data to bound the combinations $y_{7\mathrm{BBN}}/D_7$ and $y_{7\mathrm{CR}}/D_7$, respectively. The 6-to-7 ratio expected (SW) from CR nucleosynthesis is $(y_6/y_7)_{\mathrm{CR}} \leq 0.9$, leading to a bound on D_6/D_7:

$$\frac{D_6}{D_7} \lesssim 8 . \quad (11)$$

That is, the small dispersion of the Population II lithium data along with the ^{6}Li abundance limits the relative 6-to-7 depletion. We caution that this calculation relies on the measured ^{6}Li in only one star, HD 84937. We find that the same models with rotation that earlier failed to reproduce the open cluster lithium abundance patterns and that predicted too much dispersion in the Population II lithium plateau and too much absolute destruction of ^{6}Li also violate this constraint on the relative depletions of ^{6}Li and ^{7}Li. From all these (independent) constraints, a consistent picture of nonzero but limited lithium depletion in the warm, metal-poor Population II plateau stars emerges.

In conclusion, models with rotational mixing that are constrained to fit the lithium abundance patterns in open clusters require that the Sun be an anomalously fast early rotator with overdepleted lithium relative to most stars of its mass and age. Extending these same models to halo stars yields depletion patterns that can be constrained by the lithium abundances observed in these stars. The predicted dispersion in lithium abundances and the predicted ^{6}Li depletion factors are consistent with the Population II data for the same solar normalization required by the open cluster data. Thus, models that satisfy all of the above criteria suggest that halo stars must deplete their initial lithium by at least 0.2 dex but by no more than 0.4 dex. The conclusion that halo stars must deplete lithium in this range relies only on the assumption that halo stars have the same distribution of initial rotational velocities as do the open cluster stars. Alternatively, significantly more lithium might be destroyed without increasing the dispersion in the observed lithium abundances if every halo star had nearly identical angular momentum histories.

Armed with our estimate of the lithium depletion factor relevant for the Spite plateau halo stars, we may use the data to bound the primordial abundance of lithium:

$$[\mathrm{Li}]_P = [\mathrm{Li}]_{\mathrm{OBS}} + \log D_7 . \quad (12)$$

Adopting for the Spite plateau abundance $[\mathrm{Li}]_{\mathrm{OBS}} = 2.25 \pm 0.10$ and for the depletion factor $\log D_7 = 0.30 \pm 0.10$, the primordial abundance should lie within the full range $2.35 \leq [\mathrm{Li}]_P \leq 2.75$, or

$$2.2 \leq 10^{10}(\mathrm{Li/H})_P \leq 5.6 . \quad (13)$$

Here we have assumed the errors in both the observed lithium abundance and the depletion factor are uniformly distributed with a width of 0.2 dex. This results in a triangular likelihood distribution for $[\mathrm{Li}]_P$, which has a 95% confidence limit range for the log of the primordial lithium abundance only 5% smaller than the full range values we quote here. Since the shape of the distributions we assume are, at best, an approximation, we quote the full range in $[\mathrm{Li}]_P$ resulting from the convolution of the two distributions.

5. IMPLICATIONS FOR BBN

The predictions of standard BBN are uniquely determined by one parameter, the density of baryons, parameterized by η, the baryon-to-photon ratio: $\eta_{10} = 273\Omega_B h^2$ (Ω_B is the ratio of the baryon density to the critical density, and the Hubble parameter is $H_0 = 100\ h$ km s^{-1} Mpc^{-1}; $\eta_{10} = 10^{10}\eta$). For standard BBN the early universe is assumed to have been homogeneous and expanding isotropically, and the energy density at the time nucleosynthesis begins (about 1 s after the big bang) is described

by the standard model of particle physics ($\rho_{\rm tot} = \rho_\gamma + \rho_e + N_\nu \rho_\nu$, where ρ_γ, ρ_e, and ρ_ν are the energy density of photons, electrons and positrons, and massless neutrinos [one species], respectively, and N_ν is the equivalent number of massless neutrino species that in standard BBN is exactly 3). In Figure 12 the primordial abundances predicted by standard BBN are shown as a function of η. The width of each curve reflects the $\pm 2\,\sigma$ uncertainty in the predictions.

Our analysis of lithium depletion by rotational mixing, when combined with the Population II lithium data leads to a primordial lithium abundance in the range $2.2 \leq 10^{10}({\rm Li/H})_P \leq 5.6$. Compared with the predictions of standard BBN (see Fig. 12), lithium identifies two possible ranges for η: a "low-η" branch with $0.8 \leq \eta_{10} \leq 1.7$ and a "high-η" branch with $3.7 \leq \eta_{10} \leq 9.0$. Once η is identified the primordial abundances of deuterium and helium 4 (also, helium 3) follow from the predictions of standard BBN.

5.1. *Low η*

The baryon density corresponding to the low-η range is quite small: $0.003 \leq \Omega_B h^2 \leq 0.006$. If the X-ray emission from rich clusters of galaxies provides a "fair" sample of the universal fraction of baryons (White et al. 1993; Steigman & Felten 1995; Evrard 1997; Steigman, Hata, & Felten 1997), this argues strongly for a very low-density, open universe: $\Omega = \Omega_B/f_B \lesssim 0.1 h^{-1/2}$. Such a low baryon density may also be in conflict with the baryon density required to reproduce the Lyα forest data in large-scale structure simulations (Weinberg et al. 1997). This low-η range predicts a high primordial deuterium abundance ($10^5[{\rm D/H}]_P \geq 17$), which is inconsistent with the low deuterium abundance inferred for some high-redshift, low-metallicity QSO absorption systems (Tytler, Fan, & Burles 1996; Burles & Tytler 1997) but not with the high abundances inferred for some other systems (Songaila et al. 1994; Carswell et al. 1994; Rugers & Hogan 1996a, 1996b; Songaila, Wampler, & Cowie 1997; Webb et al. 1997). This low-η range corresponds to a BBN-predicted helium abundance ($Y_P \leq 0.235$), which is in excellent agreement with that inferred from emission-line observations of the low-metallicity, extragalactic H II regions (Olive & Steigman 1996; Olive et al. 1997; Hogan, Olive, & Scully 1997).

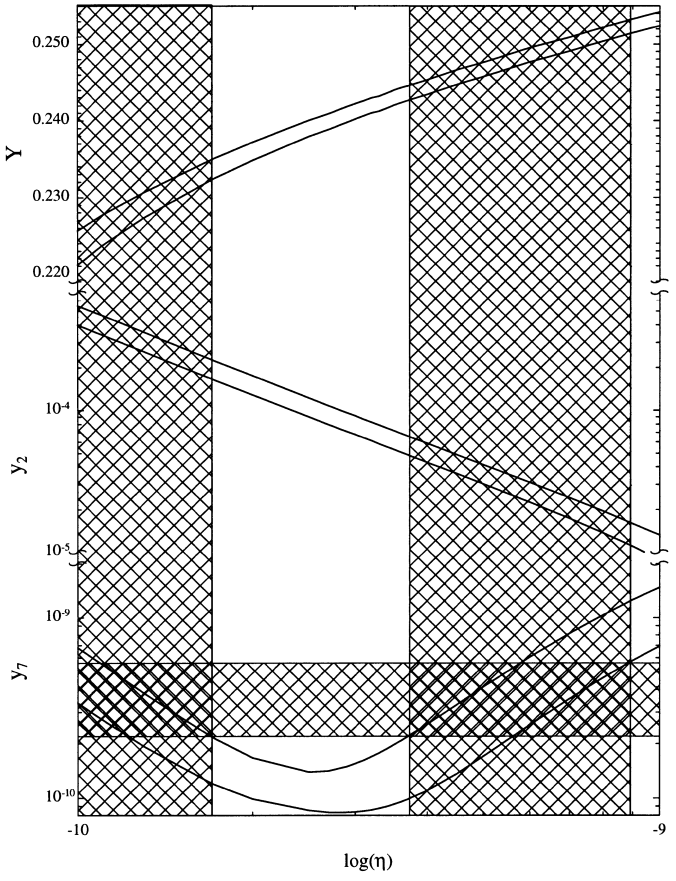

FIG. 12.—Predicted standard BBN yields (*solid lines* represent 2 σ uncertainties with three massless neutrino species) of light elements (^{4}He mass fraction, D, and ^{7}Li number fraction relative to hydrogen) as a function of η, the baryon-to-photon ratio. The primordial abundance of ^{7}Li, as inferred from lithium abundances in Population II stars and the analysis of stellar lithium depletion presented in this paper, is shown as a horizontal cross-hatched band. Vertical cross-hatched bands represent the allowed ranges of η based on the primordial abundance of ^{7}Li.

5.2. *High η*

Avoiding the minimum in the BBN lithium "valley" (see Fig. 12), this alternate branch favors a higher baryon density: $0.014 \leq \Omega_B h^2 \leq 0.033$, which, when combined with the X-ray cluster baryon fraction estimate, permits a higher total density universe: $0.2 \lesssim \Omega h^{1/2} \lesssim 0.6$. A baryon density in this range is consistent with the Lyα forest data (Weinberg et al. 1997). On this branch the primordial deuterium abundance is predicted to be smaller ($6.6 \geq 10^5[{\rm D/H}]_P \geq 1.1$), consistent with some recent estimates from high-z QSO absorbers. However, the primordial helium abundance does pose a challenge to standard BBN since $0.243 \leq Y_P \leq 0.253$ is predicted while the H II region data suggest $0.230 \leq Y_P \leq 0.238$ (but see also Izotov, Thuan, & Lipovetsky 1994, 1997 and Thuan & Izotov 1998, who derive 0.244 ± 0.002 from an independent data set).

6. SUMMARY

The lithium abundances of stars have interesting implications for cosmology and for the theory of stellar structure and evolution. The conclusions of this paper impact both of these areas. Standard stellar models implicitly assume that a variety of physical processes known to occur in real stars can be neglected; for many purposes this is a good approximation. There is now extensive evidence in Population I stars that the predictions of standard models are not in agreement with all the data. Furthermore, work from a variety of investigators on physical effects not included in the standard models has concluded that there are physically well-motivated processes that can affect the surface lithium abundances of stars. Standard models and the previous generation of nonstandard models predicted initial ^{7}Li abundances that differ by up to a factor of 10 from the same set of current Population II data, with very different implications for cosmology.

We believe that mild envelope mixing driven by rotation is the most promising candidate for explaining the complete observational picture. An improved treatment of angular momentum evolution in low-mass stars now allows us to generate stellar models with rotation that is consistent with the rotation rates observed as a function of mass and age. We have inferred the distribution of initial angular momenta in young clusters and computed the distribution of lithium depletion factors as a function of mass, composition, and age. The resulting lithium depletion pattern is in good agreement with both Population I and Population II data, and the distribution of theoretical depletion factors is

consistent with the distribution of abundances. For Population II stars in particular, the observed slope of the [Li]-$T_{\rm eff}$ relationship, the observed dispersion in abundance at fixed $T_{\rm eff}$, the existence of a small population of overdepleted stars, and the simultaneous detection of ^{6}Li and ^{7}Li in one halo star are all consistent with the predictions of the theoretical models. The primary uncertainty in the absolute depletion of ^{7}Li is the initial angular momentum of the Sun, which is used to calibrate the mixing diffusion coefficients.

We have used the observed properties mentioned above to set bounds on ^{7}Li depletion for Population II stars. Those models that fit the Population I data best predict a small but real depletion of lithium in the warm ($T_{\rm eff} \geq 5800$ K), metal-poor ([Fe/H] ≤ -1.3) Population II stars: $0.2 \leq \log D_7 \leq 0.4$. These same models are consistent with the very small observed dispersion in abundances about the plateau value and with the survival of some ^{6}Li. These depletion factors are significantly less than in previous models with rotational mixing (PDD; Chaboyer & Demarque 1994), and this difference can be directly attributed to the adoption of an improved treatment of angular momentum evolution. The uncertainties in the ^{7}Li depletion factor can be reduced by a combination of new data and improved stellar evolution models. A large set of accurate lithium abundances in old open clusters would enable us to calibrate the diffusion coefficients for mixing without relying on the solar calibration. Microscopic diffusion and rotational mixing should be considered together, although the work of Chaboyer & Demarque (1994) indicated that the predictions of such models are similar to those that include rotation alone. The observed ^{7}Li depletion pattern is relatively insensitive to the treatment of internal angular momentum transport, with a factor of 10 in the timescale corresponding to less than a 10% change in the logarithmic lithium depletion factor in the work of PDD. However, the solar rotation curve does provide evidence for angular momentum transport from mechanisms not considered in the current paper, such as magnetic fields and/or internal gravity waves. Lithium depletion in models that include these effects and hydrodynamic mechanisms should be explored. Intermediate-metallicity stars could also provide a valuable test of the dependence of lithium depletion on metal abundance.

When our constraints on lithium-depletion are combined with the abundances inferred from observations of the Spite plateau halo stars ($[{\rm Li}]_{\rm OBS} = 2.25 \pm 0.10$), we find for the range in the abundance of primordial lithium $2.35 \leq [{\rm Li}]_P \leq 2.75$ ($2.2 \leq 10^{10}[{\rm Li/H}]_P \leq 5.6$). Although lithium is not the ideal barometer, a comparison with the predictions of standard BBN identifies two options: low η and high η. The low-η branch suggests a very low baryon density, open universe, which may be in conflict with the baryon density inferred from observations of the Lyα forest. Although the helium abundance predicted for this low-η option agrees with that inferred from H II region data, the very high predicted deuterium abundance may not be consistent with observations. In contrast, the high-η branch corresponds to a baryon density consistent with the Lyα data and permits a higher density universe. In this case the predicted primordial deuterium abundance is in excellent agreement with the low-deuterium QSO data, but a considerably higher primordial helium abundance is predicted than is inferred from the observational data analyzed by both Olive & Steigman (1995) and Olive et al. (1997). The high-η branch is, however, in much better agreement with the primordial helium abundance inferred from the latest data of Izotov & Thuan (1998).

This work is supported by the Department of Energy Contract DE-AC02-76-ER01545 at The Ohio State University and NASA ATP Grant 68169492. M. H. Pinsonneault would like to acknowledge support from NASA grant NAG 5-7150 and NSF grant AST-9731621. T. P. W. thanks Sylvie Vauclair, Con Deliyannis, Corinne Charbonnel, Francois Spite, Rafael Rebolo, and Paulo Molaro for useful conversations. We also wish to thank an anonymous referee for many suggestions, which led to an improved paper.

REFERENCES

Allain, S. 1997, A&A, 333, 629
Bahcall, J. N., Pinsonneault, M. H., & Wasserberg, G. J. 1995, Rev. Mod. Phys., 67, 781
Balachandran, S. 1995, ApJ, 446, 203
Barnes, G., Charbonneau, P., & MacGregor, K. B. 1999, ApJ, 511, 466
Barnes, S., & Sofia, S. 1996, ApJ, 462, 746
Boesgaard, A. M., Deliyannis, C. P., Stephens, A., & King, J. R. 1998, ApJ, 493, 206
Boesgaard, A. M., & Trippico, M. J. 1986, ApJ, 302, L49
Bonifacio, P., & Molaro, P. 1997, MNRAS, 285, 847
Bouvier, J. 1994, in ASP Conf. Ser. 64, Eighth Cambridge Workshop on Cool Stars, Stellar Systems, and the Sun, ed. J.-P. Caillaut (San Francisco: ASP), 151
Bouvier, J., Cabrit, S., Fernandez, M., Martin, E. L., & Matthews, J. M. 1993, A&AS, 101, 485
Bouvier, J., Forestini, M., & Allain, S. 1997, A&A, 326, 1023
Brown, L., & Schramm, D. N. 1988, ApJ, 329, L103
Burles, S., & Tytler, D. 1997, AJ, 114, 1300
Cameron, A. C., Campbell, C. G., & Quaintrele, H. 1995, A&A, 298, 133
Carswell, R. F., Rauch, M., Weymann, R. J., Cooke, A. J., & Webb, J. K. 1994, MNRAS, 268, L1
Caughlin, G., & Fowler, W. A. 1988, At. Data Nucl. Data Tables, 40, 291
Chaboyer, B. C., & Demarque, P. 1994, ApJ, 433, 510
Chaboyer, B. C., Demarque, P., & Pinsonneault, M. H. 1995a, ApJ, 441, 865
———. 1995b, ApJ, 441, 876
Chaboyer, B. C., & Zahn, J.-P. 1992, A&A, 253, 173
Chandrasekhar, S., & Munch, G. 1950, ApJ, 111, 142
Charbonneau, P., & MacGregor, K. B. 1992, ApJ, 387, 639
———. 1993, ApJ, 417, 762
Charbonnel, C., Vauclair, S., & Zahn, J.-P. 1992, A&A, 255, 191
Collier-Cameron, A. C., & Li, J. 1994, MNRAS, 269, 1099
Copi, C., Schramm, D. N., & Turner, M. S. 1995a, Science, 267, 192
———. 1995b, Phys. Rev. Lett., 75, 3981
Deliyannis, C. P., Boesgaard, A. M., & King, J. R. 1995, ApJ, 452, L13
Deliyannis, C. P., Demarque, P., Kawaler, S. D., Krauss, L. M., & Romanelli, P. 1989, Phys. Rev. Lett., 62, 1583
Deliyannis, C. P., Pinsonneault, M. H., & Duncan, D. K. 1993, ApJ, 414, 740
Dring, A. R., et al. 1997, ApJ, 488, 760
Duncan, D., et al. 1997, ApJ, 488, 338
Edwards, S., et al. 1993, AJ, 106, 372
Evrard, A. E. 1997, MNRAS, 292, 289
Favata, F., Micela, G., & Sciortino, S. 1996, A&A, 311, 951
Hata, N., Scherrer, R. J., Steigman, G., Thomas, D., Walker, T. P. G., Bludman, S., & Langacker, P. 1995, Phys. Rev. Lett., 75, 3977
Hata, N., Steigman, G., Bludman, S., & Langacker, P. 1997, Phys. Rev. D, 55, 540
Hobbs, L. M., & Thorburn, J. A. 1994, ApJ, 428, L25
———. 1997, ApJ, 491, 772
Hogan, C. J., Olive, K. A., & Scully, S. 1997, ApJ, 489, L119
Izotov, Y. L., & Thuan, T. X. 1998, ApJ, 500, 188
Izotov, Y. L., Thuan, T. X., & Lipovetsky, V. A. 1994, ApJ, 435, 647
———. 1997, ApJS, 108, 1
Jones, B. F., Fischer, D., & Soderblom, D. R. 1999, AJ, 117, 307
Kawaler, S. D. 1988, ApJ, 333, 236
Keppens, R., MacGregor, K. B., & Charbonneau, P. 1995, A&A, 294, 469
Kim, Y. C., & Demarque, P. 1996, ApJ, 457, 340 (KD)
Kippenhahn, R., & Thomas, H.-C. 1970, in Stellar Rotation, ed. A. Slettebak (Dordecht: Reidel), 20

Konigl, A. 1991, ApJ, 370, L39
Krishnamurthi, A., Pinsonneault, M. H., Barnes, S., & Sofia, S. 1997, ApJ, 480, 303 (KPBS)
Krishnamurthi, A., et al. 1998, ApJ, 493, 914
Kumar, P., & Quartaert, E. J. 1996, ApJ, 475, L143
Kurucz, R. L. 1991, in Stellar Atmospheres: Beyond Classical Models, ed. L. Crivellari, I. Hubney, & D. G. Hummer (Dordrecht: Kluwer), 440
Lambert, D. L., Heath, J. E., & Edvardsson, B. 1991, MNRAS, 253, 610
Lemoine, M., Schramm, D. N., Truran, J. W., & Copi, C. J. 1996, ApJ, 478, 554
MacGregor, K. B., & Brenner, M. 1991, ApJ, 376, 204
Mestel, L. 1984, Philos. Trans. R. Soc. London A, 313, 19
Michaud, G., & Charbonneau, P. 1991, Space Sci. Rev., 57, 1
Molaro, P., Primas, F., & Bonifacio, P. 1995, A&A, 295, L47
Narayanan, V. K., et al. 1999, in preparation
Norris, J. E., Ryan, S. G., Beers, T. C., & Deliyannis, C. P. 1997, ApJ, 485, 370
Olive, K. A., Skillman, E., & Steigman, G. 1997, ApJ, 483, 788
Olive, K. A., & Steigman, G. 1995, ApJS, 97, 49
Pasquini, L., & Molaro, P. 1996, A&A, 307, 761
Patton, B., & Simon, T. 1996, ApJS, 106, 489
Peterson, R. C., Tarbell, T. D., & Carney, B. W. 1983, ApJ, 265, 972
Pilachowski, C. A., & Hobbs, L. M. 1988, PASP, 100, 336
Pinsonneault, M. H. 1997, ARA&A, 35, 557
Pinsonneault, M. H., Deliyannis, C. P., & Demarque, P. 1992, ApJS, 78, 181
Pinsonneault, M. H., Kawaler, S. D., & Demarque, P. 1990, ApJS, 74, 501
Pinsonneault, M. H., Kawaler, S. D., Sofia, S., & Demarque, P. 1989, ApJ, 338, 424
Pinsonneault, M. H., Narayanan, V. K., & Krishnamurthi, A. 1996, BAAS, 189, 7806
Rebolo, R., Molaro, P., & Beckman, J. E. 1988, A&A, 192, 192
Richard, O., Vauclair, S., Charbonnel, C., & Dziembowski, W. A. 1996, A&A, 312, 1000
Roger, F. J., & Iglesias, C. A. 1992, ApJS, 79, 507
Rugers, M., & Hogan, C. J. 1996, ApJ, 459, L1
———. 1996, AJ, 111, 2135
Ryan, S. G., Beers, T. C., Deliyannis, C. P., & Thorburn, J. A. 1996, ApJ, 458, 543
Smith, V. V., Lambert, D. L., & Nissen, P. E. 1993, ApJ, 408, 262
Soderblom, D. R., Stauffer, J. R., Hudon, J. D., & Jones, B. F. 1993a, ApJS, 85, 31
Soderblom, D. R. 1995, Mem. Soc. Astron. Italiana, 66, 347
Soderblom, D. R., et al. 1993b, AJ, 106, 1059
Songaila, A., Cowie, L. L., Hogan, C. J., & Rugers, M. 1994, Nature, 368, 599
Songaila, A., Wampler, E. J., & Cowie, L. L. 1997, Nature, 385, 137
Spite, F., & Spite, M. 1982, A&A, 115, 357
Spite, M., Francois, P., Nissen, P. E., & Spite, F. 1996, A&A, 307, 172
Spite, M., Maillard, J. P., & Spite, F. 1984, A&A, 141, 56
Stauffer, J. R., Balachandran, S. C., Krishnamurthi, A., Pinsonneault, M. H., Terndrup, D. M., & Stern, R. A. 1997, ApJ, 475, 604
Steigman, G., & Felten, J. E. 1995, Space Sci. Rev., 74, 245
Steigman, G., Fields, B. D., Olive, K. A., Schramm, D. N., & Walker, T. P. 1992, ApJ, 415, L35
Steigman, G., Hata, N., & Felten, J. E. 1997, Space Sci. Rev., 84, 31
Steigman, G., & Walker, T. P. 1992, ApJ, 385, L13
Swenson, F. J. 1995, ApJ, 438, L87
Swenson, F. J., & Faulkner, J. 1992, ApJ, 395, 654
Talon, S., & Zahn, J.-P. 1997, A&A, 329, 315
Thorburn, J. A. 1994, ApJ, 421, 318
Thorburn, J. A., Deliyannis, C. P., Rubenstein, E. P., Rich, R. M., & Orosz, J. A. 1997, in Tenth Cambridge Workshop on Cool Stars, Stellar Systems, and the Sun, in press
Thuan, T. X., & Izotov, Y. L. 1998, Space Sci. Rev., 84, 83
Tomczyk, S., Schou, J., & Thompson, M. J. 1995, ApJ, 448, L57
Tytler, D., Fan, X. M., & Burles, S. 1996, Nature, 381, 207
Vauclair, S., & Charbonnel, C. 1995, A&A, 295, 715
———. 1998, ApJ, 502, 372
Walker, T. P., Steigman, G., Schramm, D. N., Olive, K. A., & Kang, H.-S. 1991, ApJ, 376, 51
Webb, J. K., Carswell, R. F., Lanzetta, K. M., Ferlet, R., Lemoine, M., Vidal-Madjar, A., & Bowen, D. V. 1997, Nature, 388, 250
Weyman, R., & Sears, R. L. 1965, ApJ, 142, 174
White, S. D. M., Navarro, J. F., Evrard, A. E., & Frenk, C. S. 1993, Nature, 366, 429
Yang, J., Turner, M. S., Steigman, G., Schramm, D. N., & Olive, K. A. 1984, ApJ, 281, 493
Zahn, J.-P., Talon, S., & Matias, J. 1997, A&A, 322, 320
Zappala, R. R. 1972, ApJ, 172, 57